



Airborne particles in city bus: concentrations, sources and simulated pulmonary solubility

Miloš Miler

Received: 15 December 2019 / Accepted: 30 October 2020 / Published online: 11 November 2020
© Springer Nature B.V. 2020

Abstract PM₁₀ and PM_{2.5} concentrations in Ljubljana city bus were monitored during entire shift, and individual particles were morphologically and chemically characterised in order to determine PM concentration variability, particle sources, solubility in simulated pulmonary environment and effects on human health. PM measurements revealed high mean PM₁₀ (82.8 $\mu\text{g}/\text{m}^3$) and PM_{2.5} (47 $\mu\text{g}/\text{m}^3$), which were highest and most variable during rush hours with fluid traffic and lowest during traffic jams with standing vehicles. Individual particle analysis showed that airborne particles were dominated by metal-bearing phases, particularly small-sized (Cr,Mn,Zn)-bearing Fe-oxyhydroxides and Al-/Fe-Al-oxides, large (Fe,Cr,Ni)- and (Cu,Zn,Ni)-alloys, and small-sized Sb-sulphide and Ba-sulphate. Non-metallic phases were represented by (Ca,Mg)-carbonates, Al-silicates, Na-chloride and Ca-sulphate. Comparison with possible source materials (vehicle exhaust emissions, brake disc dust and road sediment) showed that primary sources of these metal-bearing phases were wear of brake discs, brake pads and tyres, and also wear of engine components and catalytic converters. Most non-metallic phases originated from resuspension of road sediment, containing road sanding materials, but also from emissions of burned fuel

and lubricating oil (Ca-sulphate). Assessment of effects on human health indicated that mean PM concentrations, which significantly exceeded daily limit values, increased mortality (by 2–3%) and morbidity (by 7–8%) risk for bus drivers. Simplified PHREEQC calculations of airborne metal-bearing phase solubility in aqueous solutions simulating pulmonary environment showed that metallic Fe, Ba-sulphate, Sb-sulphide and Al-oxide, partly also Cu-bearing metal alloys, were soluble under reducing and oxidising conditions, but released metals were removed from solution by precipitation of stable secondary metal-bearing phases.

Keywords City bus · Particulate matter concentrations · SEM/EDS characterisation · Sources · Simulated pulmonary solubility

Introduction

The urban environment in which we live today is increasingly burdened with various potentially harmful solid airborne pollutants that diminish quality of human life (Bell and Holloway 2007; Mills-Knapp et al. 2012) and also have negative influence on the environment and the rest of the ecosystems either due to their chemical composition and (in)stability in the environment or size. Many researches have

M. Miler (✉)
Geological Survey of Slovenia, Dimičeva ulica 14,
1000 Ljubljana, Slovenia
e-mail: milos.miler@geo-zs.si

established that particle pollution has a great negative impact on human health (Gilmour et al. 1996; Breed et al. 2002; Krsmanović 2003; Chen et al. 2006; Slanina 2006; Anderson et al. 2012; Son and Bell 2013; Martin et al. 2014; Kim et al. 2015; Lin et al. 2017; Miri et al. 2017; Thompson 2018; Wu et al. 2018; Deng et al. 2019). Particularly very small (micron- and submicron-sized) particles can be very reactive and potentially toxic to living organisms, due to their size, chemical composition and large specific surface area available for interactions (Rist and Hartmann 2017; Makino 2018; Khan et al. 2019). They commonly affect respiratory and cardiovascular systems (e.g. Anderson et al. 2012; Son and Bell 2013; Lin et al. 2017; Hamanaka and Mutlu 2018; Deng et al. 2019). More recently, PM has also been regarded as a potential carrier of dangerous viruses (Setti et al. 2020). Solid airborne particles often represent important carriers of potentially toxic metals, which are bound as the main constituents or trace elements in particles (Okuda et al. 2008). The toxicity of elements in particles depends on their form of occurrence (Chen et al. 2006; Sun et al. 2014), which is why it is important to determine chemical and mineral composition and morphology of individual particles. In urban environments, commuters are being increasingly exposed to constant particulate air pollution. Exposure of commuters to particle air pollution has been studied by many researchers (e.g. Alm et al. 1999; Chan et al. 2002; Tsai et al. 2008; Kongtip et al. 2012; Onat and Stakeeva 2013; Odekanle et al. 2016; Cepeda et al. 2017; Kumar et al. 2018; Correia et al. 2020). It has been shown in several studies that exposure of commuters to air pollution depends on modes of transportation (Chan et al. 2002; Tsai et al. 2008; Zuurbier et al. 2010; Moreno et al. 2015; Gokul Raj and Karthikeyan 2020). Commuters travelling by closed cabin-based road vehicles (buses, cars) are generally more exposed than those travelling by road vehicles without cabin (motorcycles and mopeds) or pedestrians and even cyclists (Adams et al. 2001, 2002; Kaur et al. 2007; McNabola et al. 2008; Boogaard et al. 2009; Zuurbier et al. 2010; Karanasiou et al. 2014; Cepeda et al. 2017; Kumar et al. 2018). Particularly vulnerable are professional city bus drivers who are directly exposed to high concentrations of small airborne particles as they spend the entire shift (8 h and more) in vehicles. The exposure of bus drivers depends on the bus routes, weather

conditions and also on the position of vehicle air intake and quality of filtration system (Zuurbier et al. 2010; Kongtip et al. 2012; Onat and Stakeeva 2013; Moreno et al. 2015).

Airborne particles are natural and anthropogenic by origin, as well as secondary authigenic particles that form in the atmosphere by chemical reactions or chemical changes of originally natural or anthropogenic solid and gaseous aerosols (e.g. Xie et al. 2009; Gieré and Querol 2010; Grobéty et al. 2010; Wang et al. 2019). The most common natural sources are weathering of bedrock and soil, resuspension and transport of desert dust, volcanic emissions, natural fires, etc. while the most important anthropogenic sources are human activities, such as industrial processes, combustion of solid and liquid fuels in furnaces and internal combustion engines, dust from traffic and salting of roads (e.g. Hodzic et al. 2007; Miler and Gosar 2009, 2013; von Glasow et al. 2009; Gieré and Querol 2010; Ny and Lee 2011; Rodríguez et al. 2011; Miler 2014; Yu et al. 2019; Teran et al. 2019). Micron-sized particles are transported from their sources by air, travelling several tens or even hundreds of kilometres before being deposited (Schöner et al. 1993; Girard 2010). Consequently, the associations of airborne solid pollutants are very diverse and complex, as they represent a mixture of natural and anthropogenic solid particles (Mudge 2008). Transformations of particles due to various processes involved during their transport or after their deposition also add to the complexity. These transformations influence chemical and physical properties of particles and consequently affect their stability and bioavailability of constituent elements (Hudson-Edwards 2003). In order to efficiently control emissions (Davis et al. 2009) and limit exposure to airborne particles, it is important to assess sources of airborne particles, natural as well as anthropogenic, which enter vehicles and contribution of these sources to health risks. No studies related to source apportionment of airborne particles that enter vehicles, their contribution and assessment of particle stability in pulmonary environment have been conducted in Slovenia yet.

The aim of our investigation was to: (1) measure airborne particle concentration inside the bus driver's cabin and their distribution with respect to time and location, (2) identify and characterise airborne particles, to which bus drivers are exposed, with regard to their physicochemical properties, (3) apportion

airborne particles according to their principal sources and (4) assess their stability and solubility in simulated pulmonary environment as an indicator of potential detrimental effects on human health.

Materials and methods

Measurements and sampling of airborne particulate matter (PM) in the bus

The measurements of airborne particulate matter (PM) concentrations were taken on 17 March 2015 between 05:26 and 11:03 h in a 24-year-old diesel bus (MAN SG 220) on a city bus line number 6 in the city of Ljubljana (Slovenia). There were 7 runs (4 in direction from location (bus stop) 1 to 26 and 3 in direction from location 26 to 1). The bus had ventilation with direct air intake fitted at the front of the bus below the windshield and was not equipped with particulate filters or air-conditioning. At the time of sampling and measurements, there were 21 (about 10%) similar buses in operation. The bus line number 6 is 22.8 km long and runs in north–south direction along high-traffic routes in Ljubljana city (Fig. 1). It is the busiest line with about 16,000,000 passengers transported yearly and has the most frequent bus traffic among all 33 bus lines in Ljubljana (Wikipedia contributors 2018). A portable dust monitor (OPC) (Grimm aerosol spectrometer model 1.109) was used for measurements and sampling. Measuring interval was 6 s, and data output (storage interval) was set at 1-min interval. Gravimetric factor (C-factor) was arbitrarily set to 1. The sample airflow was 1.2 l/min, thus 416 L of air were filtered, and the calculated weight of material collected on the filter was 42 µg. Airborne particles were collected on original Grimm PTFE (Teflon) filters with diameter of 47 mm.

Sampling of vehicle exhaust, brake disc particles and road sediment

In order to assess possible particle sources, particles emitted from exhausts of gasoline and diesel cars, dust from brake discs and road sediment were sampled. Exhaust emissions from gasoline car were sampled during 30-min drive using a special holder, on which an aluminium SEM stub with double-sided carbon tape was affixed and fitted inside the vehicle's exhaust

pipe. In diesel car, material deposited on the interior walls of the tailpipe was collected. Dust from brake discs and linings was sampled by means of SEM stub with double-sided carbon tape. Fine road sediment was collected at two locations along the bus route (near bus stops 10 and 15; Fig. 1) using a nylon scrub brush, and a composite sample of fraction < 0.125 mm was prepared for scanning electron microscopy/energy-dispersive spectroscopy (SEM/EDS).

Particle analysis

For particle analysis, the OPC filter, particles from diesel exhaust, brake disc dust and road sediment were coated with a thin layer of carbon for conductivity, while particles from gasoline vehicle emissions were not coated as they were conductive enough. All samples were analysed in backscattered electron (BSE) mode in high vacuum using scanning electron microscope JEOL JSM 6490LV, coupled with Oxford INCA Energy 350 energy-dispersive spectroscopy (EDS) system at accelerating voltages of 5–20 kV, spot size of 28–50 and working distance of 10 mm. The relative mineral and phase abundances were estimated from the distribution of constituent elements, obtained by the EDS elemental mapping of 5 (filter) and 2 (exhaust, discs and road sediment) randomly selected fields of view at magnifications of 4300 × (filter), 110 × (gasoline car), 400 × (diesel car, road sediment) and 600 × (brake discs) with an acquisition time of 700 s, by using Area Measurements tool included in the INCA Energy software (Oxford Instruments 2006). Individual particles were characterised by size, morphology and chemical composition measured by the EDS point analysis with an acquisition time of 60 s. Particle size was measured by using a measuring tool included in the JEOL SEM software (JEOL 2007). Possible metal-bearing mineral equivalents were assessed from the atomic proportions of the constituent elements, acquired by EDS point analysis and comparison with atomic proportions of constituent elements in known stoichiometric minerals, obtained from mineral databases (Anthony et al. 2009; Barthelmy 2010). The software was calibrated for quantification using premeasured universal standards included in the EDS software, according to fitted standards procedure (Goldstein et al. 2003), referenced to a Co optimisation standard.

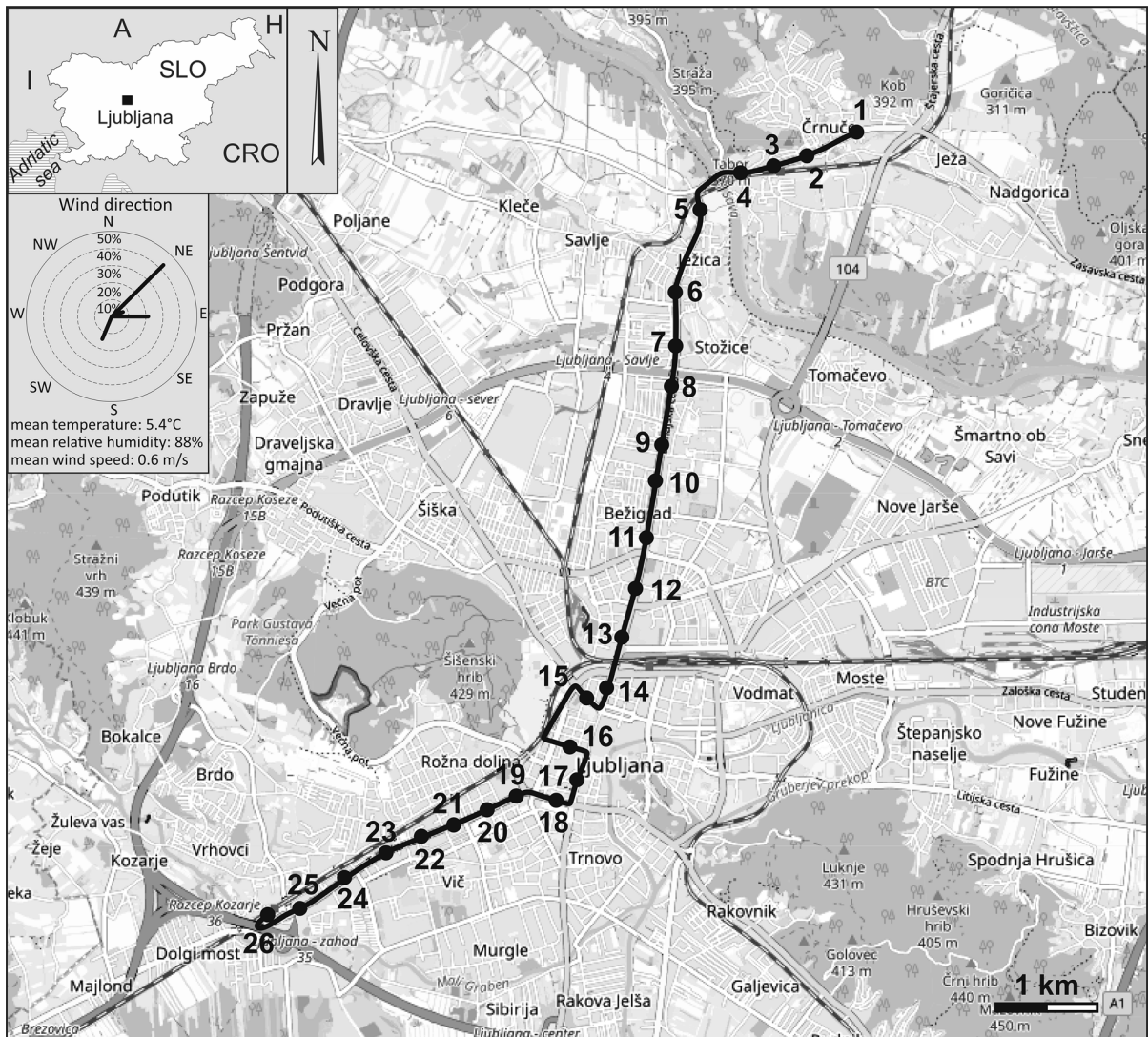


Fig. 1 Map of the studied bus line number 6 showing the route (black line) and marked bus stops (locations; black dots). ©OpenStreetMap contributors. Predominant wind directions, mean wind speed, mean temperature and mean relative humidity for the studied time period are based on data obtained by Slovenian Environment Agency (2019)

The correction of EDS data was performed on the basis of the standard ZAF-correction procedure included in the INCA Energy software (Oxford Instruments 2006).

Solubility of metal-bearing phases

The solubility of metal-bearing phases in the bus PM in simulated pulmonary environment was assessed by calculating concentrations of released metals in solution after dissolving equal amounts of metal-bearing

phases in aqueous solution under conditions similar to those in artificial lysosomal fluid (ALF) (at $T = 37\text{ }^{\circ}\text{C}$; $\text{pH} = 4.5$; $E_h = -247$ and $+247\text{ mV}$; $c(\text{Cl}^-) = 57.7\text{ mmol/l}$; $c(\text{Na}^+) = 209.6\text{ mmol/l}$; $c(\text{Ca}^{2+}) = 0.9\text{ mmol/l}$; $c(\text{Mg}^{2+}) = 0.5\text{ mmol/l}$; $c(\text{HPO}_4^{2-}) = 0.5\text{ mmol/l}$; $c(\text{SO}_4^{2-}) = 0.3\text{ mmol/l}$), according to Johnson (2003), Midander et al. (2010) and Go and Jones (2016). These calculations were carried out using PHREEQC program (version 2.14.3; Parkhurst and Appelo 1999) and a thermodynamic database LLNL.DAT.

Results and discussion

PM10 and PM2.5 concentrations in the bus

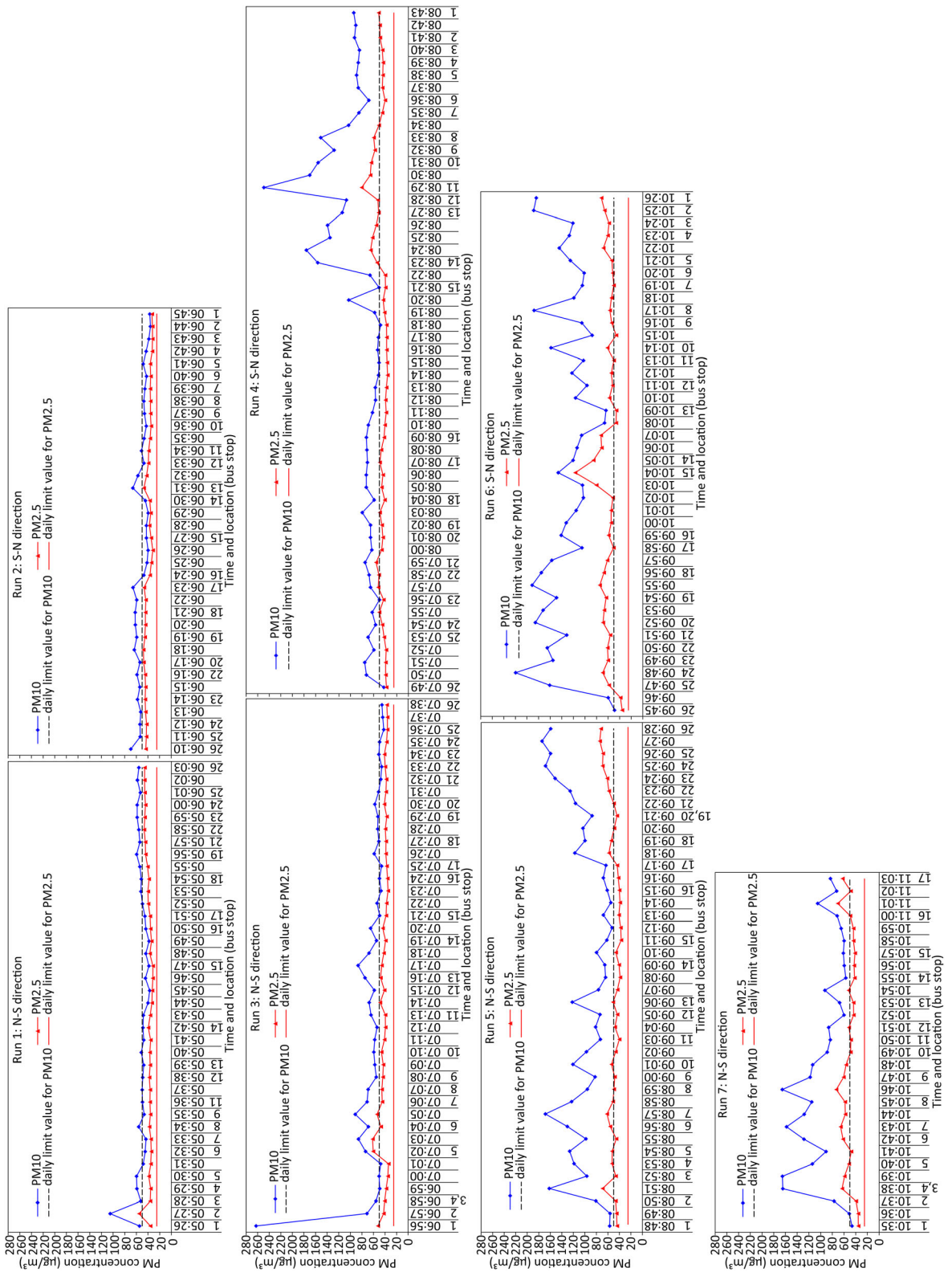
The results of measurements of airborne particles are shown in Fig. 2. The measurements during the entire shift (576 measurements) showed that the concentration of PM10 ranged between 36 and 263 $\mu\text{g}/\text{m}^3$ with a mean value of $82.8 \pm 41.9 \mu\text{g}/\text{m}^3$ (Table 1), while the concentration of PM2.5 ranged between 32 and 117 $\mu\text{g}/\text{m}^3$ with a mean value of $47.0 \pm 11.3 \mu\text{g}/\text{m}^3$ (Table 1). The ratio between mean PM2.5 and mean PM10 was 0.57, which shows that more than half of the PM10 concentration was represented by PM2.5 fraction.

Comparison with some other studies of PM10 and PM2.5 in the buses (Table 1) showed that the PM concentrations measured in our study were comparable but slightly higher than those identified by Zuurbier et al. (2010) in Arnhem, Netherlands, where mean PM10 values were $68.5 \mu\text{g}/\text{m}^3$, and by Tsai et al. (2008) in Taipei, Taiwan, where mean PM10 and PM2.5 concentrations reached $70 \mu\text{g}/\text{m}^3$ and $38.5 \mu\text{g}/\text{m}^3$, respectively. Much higher mean values were obtained in non-air-conditioned buses in Hong Kong that reached $112 \mu\text{g}/\text{m}^3$ for PM10 and $93 \mu\text{g}/\text{m}^3$ for PM2.5 (Chan et al. 2002), and in commuter buses in Istanbul, Turkey, during summer and late fall months when they reached $174 \mu\text{g}/\text{m}^3$ for PM10 and 75 to $85 \mu\text{g}/\text{m}^3$ for PM2.5 (Onat and Stakeeva 2013; Keskin and Dilmac 2017) and were particularly high during rush hours. Even higher PM10 and PM2.5 concentrations in non-air-conditioned buses were measured in Bangkok, Thailand, reaching up to 850 and $370 \mu\text{g}/\text{m}^3$, respectively (Kongtip et al. 2012).

Temporal evolution of bus PM during all 7 runs

The mean PM10 and PM2.5 concentrations and PM2.5/PM10 ratios for each run are given in Table 2. During the first two runs (run 1 and 2; Fig. 2), between 05:26 and 06:45, the PM10 concentrations were relatively low and mostly constant (Table 2). In the third run (run 3; Fig. 2), from the outskirts of Ljubljana towards the city centre, both PM10 and PM2.5 concentrations were elevated between 07:00 and 07:20, which was related to observed higher traffic density. The greater portion of PM10 during all three runs was represented by particles with a diameter

below 2.5 μm , as indicated by high PM2.5/PM10 ratio (Table 2), particularly between bus stops 18 and 26, which was probably due to high mean relative humidity (Fig. 2) and relatively thick fog that persisted in that area until 07:50. This is also consistent with findings of some previous studies (e.g. Alm et al. 1999) that high relative humidity increases the PM2.5 fraction and reduces the coarser fraction. The fourth run (run 4; Fig. 2) was characterised by generally increased but relatively constant PM10 and PM2.5 concentrations between 07:50 and 08:11. Between 08:11 and 08:18 there was a major traffic jam, during which concentration of particles with diameter between 2.5 and 10 μm decreased, but not PM2.5. This indicates that finer PM fraction is produced by vehicle exhaust emissions, while the coarser fraction could be attributed to emissions occurring when the vehicles were moving (road dust resuspension, wear of vehicle moving parts, etc.). After 08:18 the traffic jam ended and PM10 concentration increased significantly (rush hour peak in the city centre), reaching up to $250 \mu\text{g}/\text{m}^3$, while the PM2.5 reached up to $81 \mu\text{g}/\text{m}^3$. The increase in PM10 concentration was greater than increase in PM2.5 (Table 2) indicating higher portion of coarser fraction (particles between 2.5 and 10 μm) that most probably resulted from emissions of moving vehicles. There were roadworks near location 9 between 08:32 and 08:33, which caused increase in coarser fraction. After 08:36, the PM concentrations decreased somewhat towards the outskirts of Ljubljana and remained constant until 08:43 (the end bus stop). During the fifth run (run 5; Fig. 2), the PM10 and PM2.5 concentrations varied from 52 to $174 \mu\text{g}/\text{m}^3$ with a mean of $101 \mu\text{g}/\text{m}^3$ and from 37 to $74 \mu\text{g}/\text{m}^3$ with a mean of $50 \mu\text{g}/\text{m}^3$, respectively. At the beginning of run 5, between 08:50 and 09:07, the traffic flow was fluid and the PM concentrations were very high mostly on the account of coarser PM fraction (particles between 2.5 and 10 μm). After 09:07, the concentrations, particularly of coarser PM fraction, began to decrease and the traffic became less dense at about 09:11 (location 15). Between 09:17 and 09:28, the coarser portion of PM10 began to increase again, which was rather surprising as the traffic was normal. This increase could be due to somewhat higher number of passengers travelling towards the end bus stop 26. Sixth run (run 6; Fig. 2) was again characterised by generally high PM10 concentrations with very high portion of coarser fraction between 2.5 and



◀ **Fig. 2** PM10 and PM2.5 concentrations measured at 1-min storage interval during all 7 runs on a Ljubljana city bus line number 6. The daily limit values for PM10 are taken from WHO (2006) and Official Gazette RS (2011), and daily limit values for PM2.5 are taken from WHO (2006)

10 µm (Table 2), which began to gradually decrease between 09:55 and 10:09. At 10:04, there was a pronounced increase in PM2.5 in the strict centre of Ljubljana reaching up to 117 µg/m³, whose cause could not be exactly determined but could perhaps be attributed to vehicle exhaust emissions and poor ambient air ventilation at that time. Between 10:09 and 10:26 (end bus stop), the PM10 was fluctuating but

gradually increasing, especially the coarser fraction. At 10:16, there was another peak near the roadworks at location 9. In the final run (run 7; Fig. 2), the PM10 concentrations were still very variable until 10:49 when they began to decrease. Although the mean relative humidity in outdoor air was very high (88%) during all seven runs and mean wind speed was practically negligible (0.6 m/s) (Fig. 2), PM was mostly represented by coarser fraction (particles with diameter between 2.5 and 10 µm), particularly in the last four runs, which is in contrast to findings of Alm et al. (1999). In contrast to findings of Tsai et al. (2008), who noticed a significant increase in PM10 and PM2.5 during opening of bus doors at bus stops, opening doors at each bus stop in our study did not

Table 1 Comparison with other studies of PM in buses

Study	Location	Bus ventilation type	Particulate matter	Mean PM concentration (µg/m ³)
This study	Ljubljana, Slovenia	non-A/C	PM10	82.8
			PM2.5	47
Chan et al. (2002)	Hong Kong	non-A/C	PM10	112
			PM2.5	93
Tsai et al. (2008)	Taipei, Taiwan	A/C	PM10	70
			PM2.5	38.5
Zuurbier et al. (2010)	Arnhem, Netherlands	A/C	PM10	68.5
Kongtip et al. (2012)	Bangkok, Thailand	non-A/C	PM10	850
			PM2.5	370
Onat and Stakeeva (2013)	Istanbul, Turkey	non-A/C	PM2.5	85
Keskin and Dilmac (2017)	Istanbul, Turkey	non-A/C	PM10	174
			PM2.5	75

A/C air-conditioned

non-A/C non-air-conditioned

Table 2 Mean PM10 and PM2.5 concentrations (µg/m³), PM2.5/PM10 ratios and duration times for each run on a Ljubljana city bus line number 6

Run	PM10 concentration		PM2.5 concentration		PM2.5/PM10	Run duration time (min)
	PM10 _{avg}	PM10 _{std}	PM2.5 _{avg}	PM2.5 _{std}		
Run 1	51.4	10.9	38.7	5.1	0.75	37
Run 2	50.4	9.1	39.5	5.1	0.78	35
Run 3	63.1	33.4	41.8	6.3	0.66	42
Run 4	86.1	40.0	47.0	8.9	0.55	54
Run 5	101.0	36.6	50.2	9.9	0.50	40
Run 6	130.5	39.3	60.4	13.6	0.46	41
Run 7	94.7	36.2	51.7	10.1	0.55	28

have significant effect on the PM concentrations. At some bus stops, the concentrations increased, while at others they decreased. This could be due to different bus dwell times at different bus stops, which were much shorter than a minute at some bus stops, particularly outside rush hour and outside city centre. Since measurement storage interval was 1 min, it is possible that concentration changes were simply not registered. It also depends on ambient PM₁₀ and PM_{2.5} concentrations at each bus stop. At lower ambient concentrations, the bus concentrations could also decrease due to ventilation.

Comparison of hourly PM₁₀ concentrations in the bus with hourly concentrations in ambient air (Slovenian Environment Agency 2015), obtained from automatic monitoring station situated 300 m east of location 12, showed relatively good match in the rising concentration trend between 06:00 and 08:00 (Fig. 3). However, PM₁₀ increased significantly in the bus between 08:00 and 10:00, while in the ambient air they decreased. This shows the prevailing influence of local road traffic emissions on the air quality in the bus during this time period. The calculated ratio between mean daily PM_{2.5} (29 µg/m³) and PM₁₀ (42 µg/m³) concentration in ambient air (Slovenian Environment Agency 2015) was 0.69, which is higher as compared with the ratio of 0.57 in the bus PM, and implies larger portion of coarser PM fraction in the bus PM, most probably due to more direct intake of larger resuspended particles from the road. This is consistent with findings of Gehrig and Buchmann (2003) that the PM_{2.5}/PM₁₀ ratio of 0.59 shows strong influence of coarse particles from traffic-induced mechanical abrasion and dust resuspension. Finer particles generally have longer retention times in the air than coarser particles, thus resulting in increase in PM_{2.5}/PM₁₀ ratio with the distance from the major roads. However, the PM_{2.5}/PM₁₀ ratio in the bus can also be higher, as shown by Chan et al. (2002) who ascribed high ratio of 0.68 to vehicle exhaust emissions.

Relative mineral and phase abundances in investigated samples

The EDS element maps showed that the airborne particles collected on OPC filter are predominantly composed of metal-bearing phases (84%) and 17% of non-metallic phases (Table 3). Metal-bearing phases are represented by Fe-oxyhydroxides (81%) and minor

metal-bearing phases, which are alloys of Cu–Zn, Ni–Cu and metallic Cu with minor content of S and Ba, alloys of Fe–Cr–Ni, Cr–Ni and metallic Ni, Al-oxide, Ti-oxides, Pb-oxide/carbonate and Ba-sulphate, which together make up 2.6% of the sample. Non-metallic phases comprise (Ca,Mg)-carbonates (10%), such as dolomite and calcite, and various Al-silicates (about 5%), including mica, feldspars and quartz (Table 3). Other non-metallic phases are Na-chloride (halite) (1%) and Ca-sulphate (anhydrite or gypsum) (0.2%). Gasoline and diesel car exhaust emissions consist predominantly of C-bearing particles, such as porous sponge-like soot particles, between 80% (gasoline car) and 99% (diesel car). Gasoline car emissions are also characterised by relatively high amount of Al-oxide (12%) and minor amounts of Ca–Zn-phosphates with variable contents of Fe and S and minor contents of Cu (3.6%), Ca-sulphate (0.4%) and amorphous Ca–Mg-silicate (fragments of smooth fibres of high-temperature silicate wool) (0.6%). Other minor metal-bearing phases are alloys of Fe–Cr–Ni, Cr–Ni and metallic Ni and Fe-oxyhydroxide each representing 0.9% of the sample. Minor amounts of Al-silicates (0.5%), Fe-oxyhydroxides (0.2%) and Ca-sulphates (0.1%) were found in diesel car exhaust samples. Brake disk samples are characterised by high amount of Fe-oxyhydroxides (over 90%), minor amounts of Fe-sulphide (pyrite) (over 1%), Ba-sulphate (0.7%), Al-oxide (0.4%), but also non-metallic phases quartz and Al-silicates (about 4%), (Ca,Mg)-carbonates (3%) and Na-chloride (0.2%).

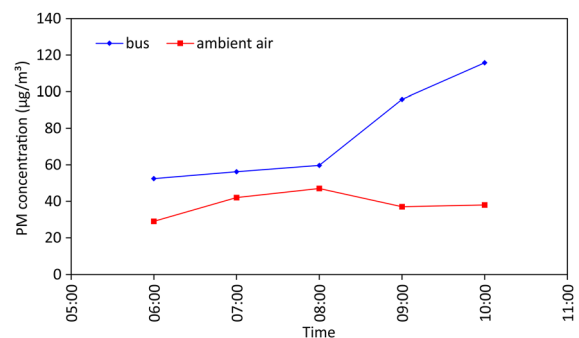


Fig. 3 Comparison between mean hourly PM₁₀ concentrations in the bus and ambient air. The ambient air data were obtained from automatic monitoring station (Slovenian Environment Agency 2015)

Table 3 Relative mineral and phase abundances (%) in investigated OPC filter, gasoline and diesel car emissions, dust from brake discs and road sediment

Mineral/phase	Samples				
	OPC filter (%) 4300 ×	Gasoline car (%) 110 ×	Diesel car (%) 400 ×	Brake disc (%) 600 ×	Road sediment (%) 400 ×
C-bearing	–	81.0	99.2	–	–
C-S-bearing	–	–	–	–	1.8
(Ca,Mg)-carbonates	10.0	–	–	3.0	68.1
Al-silicates + quartz	5.3	–	0.5	3.9	21.4
Ca-Mg-Si-O	–	0.6	–	–	–
Na-Cl	1.0	–	–	0.2	–
Ca-S-O	0.2	0.4	0.1	–	–
Ca-Zn-P-(S)-(Fe)-O(Cu)	–	3.6	–	–	–
Fe-S	–	–	–	1.3	–
Fe-Cr-Ni/Cr-Ni/Ni	0.3	0.9	–	–	1.8
Cu(S,Ba)/Cu-Zn/Ni-Cu	0.6	–	–	–	0.1
Al-O/Fe-Al-O	0.9	12.4	–	0.4	0.1
Fe-O	81.0	0.9	0.2	90.6	5.9
Ti-O	0.5	–	–	–	0.5
Ba-S-O	0.1	–	–	0.7	0.1
Pb-(C)-O	0.2	–	–	–	0.2

– not identified

Characteristics of individual particles and phases

For a detailed characterisation of individual phases, individual particle analysis was employed. Identified phases in the bus PM (OPC filter), in gasoline and diesel car emissions, dust from brake discs and road sediment together with their grain sizes and abundances are presented in Table 4. Images of representative phases are shown in Figs. 4, 5, 6 and 7.

Phases in the bus PM

In the bus PM, 15 different types of metal-bearing phases were identified (Table 4), which were classified into 3 groups.

The most abundant group are metal-bearing oxides/oxyhydroxides represented by pure Fe-oxyhydroxides (Fig. 4a), Fe-oxyhydroxides with minor contents of Cr, Mn and Zn (Fig. 4b), Fe-oxyhydroxides with minor Cu, Zn and Sn, Ca-ferrites with minor content of Cr, spherical Fe-Zn- and Cr-Fe-oxides, Al- and Fe-Al-oxides (Fig. 4c) and Ti-oxides. Fe-oxyhydroxides with minor contents of Cr, Mn and Zn occur mostly as

anhedral platy fragments with striated surfaces, but also as porous agglomerates of minute crystallites. Ca-ferrites with minor content of Cr are represented by anhedral, porous and flat particles. Pure Fe-oxyhydroxides (probably minerals goethite or lepidocrocite) are characterised by elongated and coiled shavings, while Al-oxides (mineral corundum) and Fe-Al-oxides (probably mineral hercynite) are anhedral and flat. Ti-oxides (mineral rutile) occur as euhedral rod-like crystals and Fe-oxyhydroxides with minor Cu, Zn and Sn as anhedral agglomerate of minute crystallites. Spherical Fe-Zn-oxides (possibly mineral franklinite) and Cr-Fe-oxides are very small and have smooth surfaces. All these phases are very small. Their mean grain sizes range from 1.2 to 5.5 µm.

The second group are metal alloys represented by alloys of Cu-Zn (Fig. 4d), Ni-Cu and metallic Cu with minor content of S and Ba, metallic Fe and Fe with minor contents of Cr, Ni and Cu (Fig. 4e), alloys of Fe-Cr-Ni, Cr-Ni and metallic Ni (Fig. 4f), and Ni-phosphide (Fig. 4g). All of the metal alloys occur as elongated angular and lamellar shavings with either smooth or striated and imbricated surfaces. Some of

Table 4 Number (n), mean size (d_{avg}) and standard deviations (std.) in μm of identified phases on OPC filter, gasoline and diesel car emissions, dust from brake discs and road sediment

Phase	Samples														
	OPC filter			Gasoline car			Diesel car			Brake disc			Road sediment		
	4300 ×			110 ×			400 ×			600 ×			400 ×		
	n	d_{avg}	std	n	d_{avg}	std	n	d_{avg}	std	n	d_{avg}	std	n	d_{avg}	std
Fe/Fe(Cr,Ni,Cu)	8	7.7	8.3	1	21.3	n.d	–	–	–	3	2.8	1.6	1	19.3	n.d
Fe–Cr–Ni/Cr–Ni/Ni	6	25.8	14.2	3	55.3	51.1	1	1.8	n.d	–	–	–	1	98.9	n.d
Ni–P	1	78.6	n.d	–	–	–	–	–	–	–	–	–	–	–	–
Cu(S,Ba)/Cu–Zn/Ni–Cu	14	30.4	48.1	2	27.2	29.6	–	–	–	–	–	–	1	16.6	n.d
Sb/Sb-S	2	5.1	1.1	–	–	–	–	–	–	–	–	–	–	–	–
Fe–O	3	2.0	0.1	–	–	–	5	3.1	1.4	2	4.6	1.1	6	21.7	16.8
Fe–O(Cr,Mn,Zn)	15	5.5	3.9	–	–	–	–	–	–	–	–	–	4	22.8	21.2
Fe–O(Cu,Zn,Sn)	1	3.3	n.d	–	–	–	–	–	–	–	–	–	13	5.3	3.3
Fe–O(Zr,Cu,Ba)	–	–	–	–	–	–	–	–	–	2	7.7	3.8	–	–	–
Fe–Cr–O(Zn)	–	–	–	1	86.7	n.d	–	–	–	–	–	–	–	–	–
Fe–V–O(Cu,Nb,Cr)	–	–	–	–	–	–	–	–	–	–	–	–	1	2.4	n.d
Fe–Ni–O	–	–	–	–	–	–	1	1.3	n.d	–	–	–	–	–	–
Fe–O–S	2	8.1	0.2	–	–	–	1	3.9	n.d	–	–	–	–	–	–
Ca–Zn–P–(S)–(Fe)–O(Cu)	–	–	–	6	51.4	40.0	–	–	–	–	–	–	–	–	–
Ca–Fe–O(Cr)	4	3.0	0.7	–	–	–	–	–	–	–	–	–	–	–	–
Spher. Fe–Zn–O	1	1.2	n.d	–	–	–	–	–	–	–	–	–	–	–	–
Spher. Cr–Fe–O	1	1.7	n.d	–	–	–	–	–	–	–	–	–	–	–	–
Spher. Fe–Al–O	–	–	–	1	41.3	n.d	–	–	–	–	–	–	–	–	–
Spher. Ni–O	–	–	–	1	12.5	n.d	–	–	–	–	–	–	–	–	–
Spher. Pb–Bi	–	–	–	1	4.3	n.d	–	–	–	–	–	–	–	–	–
Spher. Ca–P–Zn–O(Cu)	–	–	–	4	27.3	4.4	–	–	–	–	–	–	–	–	–
Al–O/Fe–Al–O	3	2.3	1.1	4	110.6	74.2	–	–	–	1	14.4	n.d	1	13.1	n.d
Fe–Sb–Al–O(Cu,Zn)	–	–	–	–	–	–	–	–	–	–	–	–	1	13.7	n.d
Ba–Al–P–O	–	–	–	1	10.4	n.d	–	–	–	–	–	–	–	–	–
Ca–Ti–O	–	–	–	–	–	–	–	–	–	–	–	–	2	25.1	5.5
Ti–O	1	4.0	n.d	–	–	–	–	–	–	–	–	–	2	7.7	5.6
Ba–S–O	1	1.8	n.d	–	–	–	–	–	–	5	5.0	2.4	3	7.8	8.1
Fe–S	–	–	–	–	–	–	–	–	–	2	9.1	3.0	–	–	–
Ca–Mg–Si–O	–	–	–	3	82.0	22.7	–	–	–	–	–	–	–	–	–
Zr–Si–O	–	–	–	–	–	–	–	–	–	–	–	–	1	2.9	n.d
C–S-bearing	–	–	–	–	–	–	–	–	–	–	–	–	6	38.8	14.7
Total n	63			28			8			15			43		

n.d. not determined

– not determined

them are partly corroded, particularly metallic Fe and Fe with minor contents of Cr, Ni and Cu, and alloys of Cu–Zn (brass), Ni–Cu (cupronickel) and metallic Cu

with minor content of S and Ba. Ni-phosphide contains inclusions of Cu–Zn alloy. The mean grain sizes of these alloys are very large and range from 8 to 79 μm .

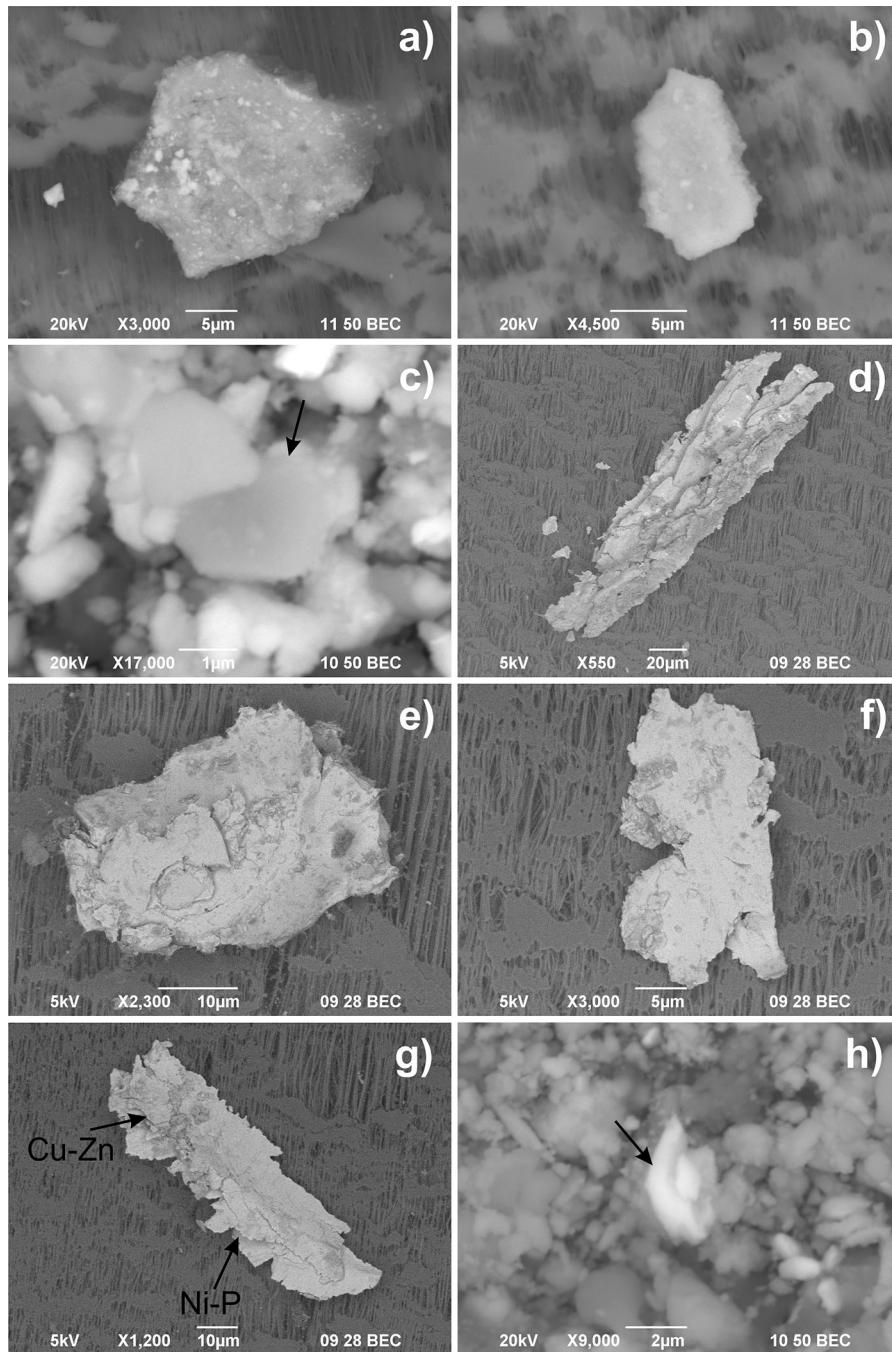


Fig. 4 SEM (BSE) images of metal-bearing phases in the bus PM: **a** Pure Fe-oxyhydroxide; **b** Fe-oxyhydroxide with minor content of Cr, Mn and Zn; **c** Al-oxide; **d** Cu–Zn alloy; **e** Fe with

minor contents of Cr, Ni and Cu; **f** Metallic Ni; **g** Ni-phosphide associated with Cu–Zn alloy (brass); **h** Sb-sulphide (arrow)

According to grain sizes and standard deviation, these phases are very poorly sorted.

The third group are sulphides and sulphates, which comprise pure Fe-oxyhydroxy sulphates, Sb-sulphide

(Fig. 4h), including metallic Sb, and Ba-sulphate. Pure Fe-oxyhydroxy sulphates (possibly mineral schwertmannite) are angular and thin with corroded surfaces and are most probably weathering products of

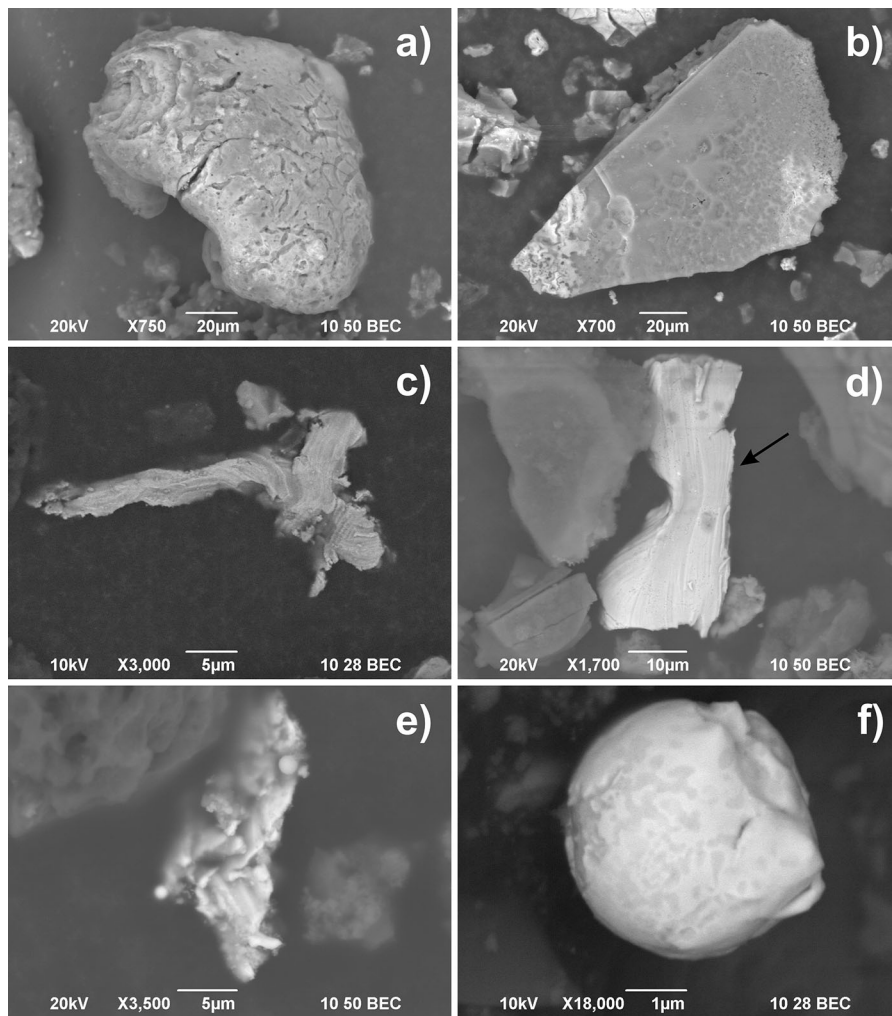


Fig. 5 SEM (BSE) images of metal-bearing phases in gasoline car exhaust emissions: **a** Ca–Zn-phosphates with variable contents of Fe and S and minor contents of Cu; **b** Al-oxide;

c Fe–Cr–Ni alloy; **d** Cu–Zn alloy (arrow); **e** Fe with minor contents of Cr, Ni and Cu; **f** spherical Pb–Bi alloy

oxidation of Fe-sulphides, while Sb-sulphide (mineral stibnite) and metallic Sb, and Ba-sulphate (mineral barite) occur as angular platy and rhomb-like or massive particles. The mean grain sizes of these phases range from 1.8 to 8 μm .

Phases in gasoline car emissions

In gasoline car emissions, 11 different types of metal-bearing phases were identified (Table 4) and classified into 3 groups. Four types of these metal-bearing phases are the same as those identified in the bus PM, particularly metal alloys and Al- and Fe–Al-oxides.

The most abundant is a group of phosphates, which are represented by Ca–Zn-phosphates with variable contents of Fe and S and minor contents of Cu (Fig. 5a), and Ba–Al-phosphate. Ca–Zn-phosphates (possibly mineral scholzite) mostly occur as rounded corroded particles or angular porous sponge-like particles with partially melted crystallites, but also as spheres with smooth surface and inclusions of Cu-sulphide with minor content of Ag. Ba–Al-phosphate forms anhedral and sponge-like porous particle with partially melted crystallites. The mean grain sizes of these phases range from 10 to 51 μm .

The second group comprises metal-bearing oxides/oxyhydroxides, which are Al- and Fe–Al-oxides

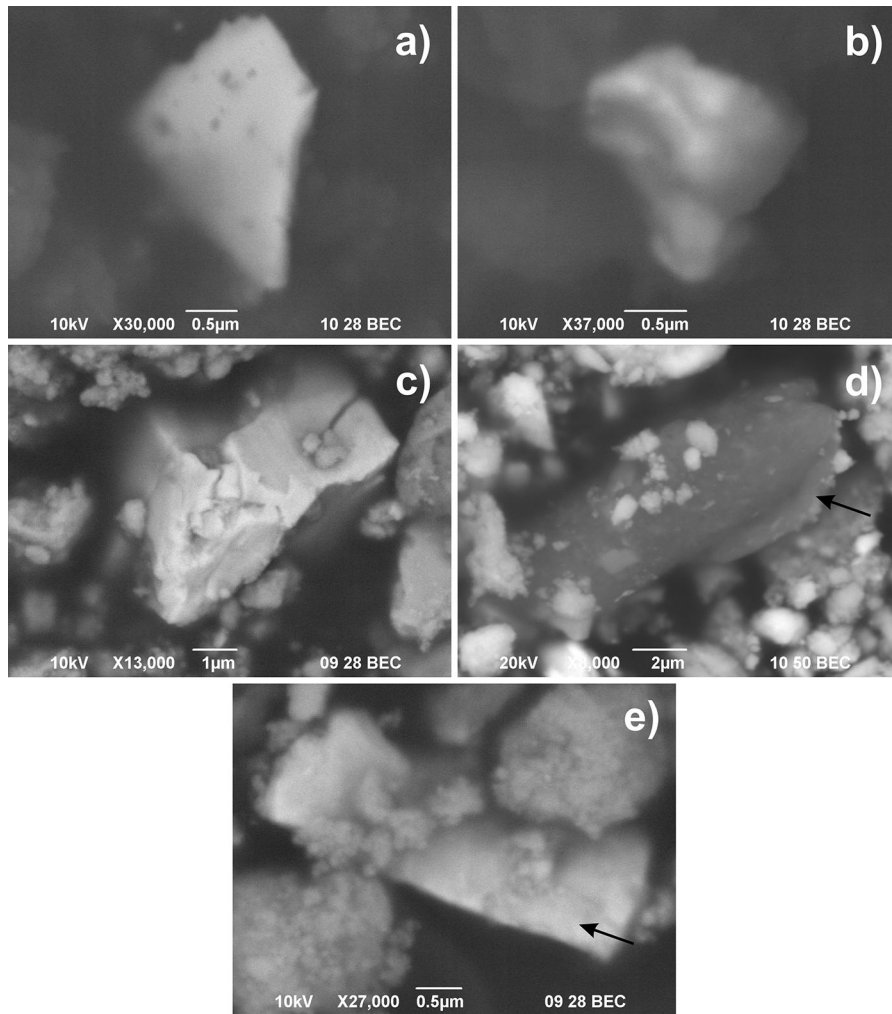


Fig. 6 SEM (BSE) images of metal-bearing phases in diesel car exhaust (a–b) and brake disc dust (c–e): **a** Pure Fe-oxyhydroxide; **b** Fe–Cr–Ni alloy; **c** Ba-sulphate; **d** Al-oxide (arrow); **e** Metallic Fe (arrow)

(Fig. 5b), Fe–Cr-oxides with minor content of Zn, and spherical Ni-oxides. Al- and Fe–Al-oxides occur as anhedral and platy fragments with corroded surface, sometimes also with shrinkage cracks, and as spherical porous agglomerate of micron-sized particles. Fe–Cr-oxides with minor content of Zn are anhedral and platy with porous surface due to oxidation. Spherical Ni-oxides have skeletal surface composed of micron-sized amorphous particles. The mean grain sizes of these phases span over wide range from 12 to 111 µm.

The third group are metal alloys represented by Fe–Cr–Ni (Fig. 5c), Cr–Ni and metallic Ni, alloys of Cu–Zn (Fig. 5d), Ni–Cu and metallic Cu with minor content of S and Ba, metallic Fe and Fe with minor contents of Cr, Ni and Cu (Fig. 5e), and spherical Pb–

Bi alloy (Fig. 5f). All of these alloys form elongated and sometimes rounded anhedral shavings with striated surfaces, with the exception of spherical Pb–Bi alloy, which has relatively smooth surface indicating partial melting. High standard deviation of grain sizes (Table 4), which range between 4 and 55 µm, indicates that these phases are poorly sorted.

Phases in diesel car emissions

Metal-bearing phases in diesel car emissions are relatively scarce. Only 4 different types were identified (Table 4) and classified into 3 groups, among which 3 types were the same as those identified in the

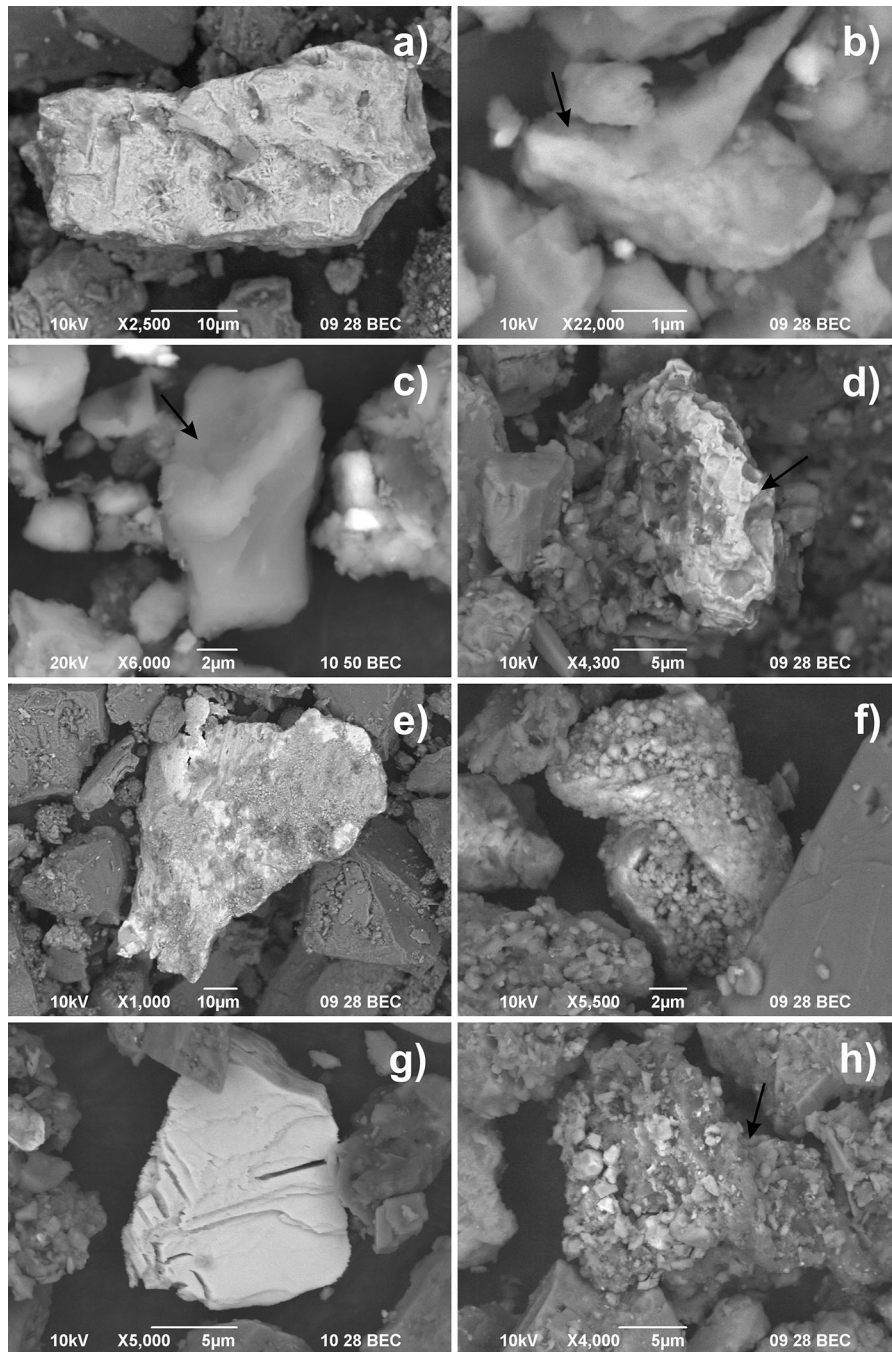


Fig. 7 SEM (BSE) images of metal-bearing phases in road sediment: **a** Pure Fe-oxyhydroxide; **b** Fe-oxyhydroxide with minor content of Cr, Mn and Zn (arrow); **c** Al-oxide (arrow);

d Metallic Fe; **e** Fe–Cr alloy; **f** Cu–Zn alloy; **g** Ba-sulphate; **h** C–S-rich particles (tyre fragments) with inclusions of various metal-bearing phases

bus PM (metal alloys, pure Fe-oxyhydroxides and pure Fe-oxyhydroxy sulphates).

The group of metal-bearing oxides/oxyhydroxides includes pure Fe-oxyhydroxides (Fig. 6a) and Fe–Ni-

oxides, while other types of metal-bearing phases belong to metal alloy group (Fe–Cr–Ni (Fig. 6b), Cr–Ni and metallic Ni) and to group of sulphides and sulphates (pure Fe-oxyhydroxy sulphates). All these

phases occur as massive angular grains, but also as thin fragments with smooth surfaces. The mean grain sizes of all these phases are very small, ranging from 1.3 to 4 μm .

Phases in brake disc dust

In brake disc dust, 6 types of metal-bearing phases were recognised (Table 4) and classified into 3 groups. Four types of these phases are the same as those in the bus PM, including metallic Fe and Fe with minor contents of Cr, Ni and Cu, pure Fe-oxyhydroxides, Al- and Fe–Al-oxides and Ba-sulphates.

The more abundant group is a group of sulphides and sulphates represented by Fe-sulphide (mineral pyrite or marcasite) and Ba-sulphate (Fig. 6c), which usually contains minor contents of Sr. They occur as massive and angular fragments with sometimes corroded surface. Their mean grain size ranges between 5 and 9 μm .

The second group comprises metal-bearing oxides/oxyhydroxides with pure Fe-oxyhydroxides, Al- and Fe–Al-oxides (Fig. 6d) and Fe-oxyhydroxides with minor contents of Zr, Cu and Ba. These phases occur as anhedral porous agglomerates or fragments of thin crusts with smooth surface, but also as elongated and partly rounded fragments. The mean grain size ranges from about 5 to 14 μm .

The group of metal alloys is represented by elongated angular fragment of metallic Fe (Fig. 6e) and Fe with minor contents of Cr, Ni and Cu and grain size of about 3 μm .

Phases in road sediment

Investigated road sediment contains a variety of metal-bearing phases. Fourteen types of metal-bearing phases were recognised, 9 of which were also identified in the bus PM (Table 4).

The most abundant is a group of metal-bearing oxides/oxyhydroxides, represented by Fe-oxyhydroxides with minor Cu, Zn and Sn, pure Fe-oxyhydroxides (Fig. 7a), Fe-oxyhydroxides with minor contents of Cr, Mn and Zn (Fig. 7b), Ca–Ti-oxides (perovskite), Ti-oxides, Fe–V-oxides with minor contents of Cu, Nb and Cr, Al- and Fe–Al-oxides (Fig. 7c) and Fe–Sb–Al-oxides with minor Cu and Zn. Fe-oxyhydroxides with minor Cu, Zn and Sn occur as individual elongated platy shavings, as massive angular inclusions in C–S-

rich particles (tyre fragments) or as porous grains composed of minute crystallites. Pure Fe-oxyhydroxides, Fe-oxyhydroxides with minor contents of Cr, Mn and Zn, and Al- and Fe–Al-oxide occur as massive angular grains or angular fragments of thin crusts. Also Ca–Ti-oxides can be found as submicron inclusions in C–S-rich particles, while Ti-oxides form angular lamellar grains. Fe–V-oxide with minor contents of Cu, Nb and Cr is anhedral and partially rounded. Fe–Sb–Al-oxide with minor Cu and Zn is a sub-rounded aggregate of submicron crystallites and Al-oxide matrix. The mean grain sizes of these phases range from 2.4 to 25 μm .

The metal alloys group consists of individual grains of metallic Fe (Fig. 7d) and Fe with minor contents of Cr, Ni and Cu, alloys of Fe–Cr–Ni (Fig. 7e), Cr–Ni and metallic Ni, and alloys of Cu–Zn (Fig. 7f), Ni–Cu and metallic Cu with minor content of S and Ba. They occur either as massive angular grains with partially melted surface and corrosion pits or as subangular platy shavings with partly striated and oxidised surface. Their grain sizes range between 17 and 99 μm .

In the group of sulphides and sulphates, Ba-sulphate (Fig. 7g) is present, which occurs as angular porous grains with corrosion pits or massive grains with corrosion cracks and distinct cleavage with mean grain size of about 8 μm .

The group of silicate is represented only by individual grain of Zr-silicate (mineral zircon), occurring as euhedral inclusion in C–S-rich particle (tyre fragment) (Fig. 7h) with size of about 3 μm .

Sources of particles and phases in bus PM

According to phase abundances (Tables 3, 4), the composition of the material on OPC filter (bus PM) corresponds well to the composition of road sediment and also of brake disc dust. The origin of (Ca,Mg)-carbonates and Al-silicates, and also Na-chloride was attributed to resuspension of road sediment as these phases are present also in road sediment where their abundances are equal to or higher than those found in bus PM (Table 3). These phases are also common in materials used for sanding of roads in the winter (Šemeš Lesjak 2014; Kupiainen et al. 2016). A major source of Ca-sulphates, which were found in bus PM as well as in gasoline and diesel car exhausts, is most likely direct emissions from gasoline and diesel exhaust

systems due to burning of fuel and lubricating oil (van Setten et al. 2001; Dallmann et al. 2014). The morphology of pure Fe-oxyhydroxides in bus PM is typical of abrasion processes; however, it differs from the morphology of Fe-oxyhydroxides in other media. According to particle morphology and their presence in bus PM and road sediment, the most important cause of Fe-oxyhydroxides with minor contents of Cr, Mn, Zn, Cu and Sn in bus PM seems to be resuspension of road sediment, in which the residence time of Fe-oxyhydroxides was long enough for them to adsorb other potentially toxic metals or for oxidation of metal alloys and metal-bearing sulphides to take place. The most probable primary source of these phases and metals, including pure Fe-oxyhydroxides, is wear of brake discs and brake pads (Kukutschová et al. 2011; Amato et al. 2012; Grigoratos and Martini 2015) but could also be wear of tyres (Evans and Evans, 2006). Al- and Fe–Al-oxides are most abundant in gasoline car emissions (Tables 3, 4) and are morphologically similar to those found in bus PM and brake disc dust. Al-oxides can be formed and emitted during engine wear (Kaiser and Dutta 2014) and are also used as washcoats in catalytic converters (Ravindra et al. 2004). However, they are also present in brake pads as friction materials, together with metallic Fe (Amato et al. 2012; Grigoratos and Martini 2015); thus, they could originate both from wear of engine, catalytic converters and brake pads. Ti-oxides and Pb-oxide/carbonate are also most abundant in the bus PM and road sediment, in addition, Ti-oxides have similar morphologies in both media. As Ti-oxides and Pb-oxide/carbonate are present in white and yellow pigments used in road marking paint (Gottesfeld 2015; Naidoo and Steyn 2018), their origin is mostly road marking paint, but natural sources of Ti-oxides, such as soil resuspension, are also possible. Metallic Fe and Fe with minor contents of Cr, Ni and Cu found in bus PM are similar in morphology to those in gasoline car emissions and dust from brake discs, but differ from those in road sediment. The probable sources are thus wear of brake discs and brake pads and also exhaust emissions (wear of engine parts), as these phases are commonly used in automotive industry (Amato et al. 2012; Saha Podder and Bhanja 2013). Alloys of Cu–Zn, Ni–Cu, metallic Cu with minor content of S and Ba, alloys of Fe–Cr–Ni, Cr–Ni and metallic Ni are most abundant in bus PM, gasoline car emissions and road sediment (Tables 3, 4) and are

morphologically very similar in all media. Their morphology is typical of mechanical abrasion and can result from wear of brake discs and brake pads (Kukutschová et al. 2011), engine components (Saha Podder and Bhanja 2013) as well as from wear of catalytic converters, as Ni–Cu alloys have been reported to be used in catalytic converters (Bernstein et al. 1973). Fe-oxyhydroxy sulphates were found only in bus PM and diesel car exhaust. According to their morphology, they could represent oxidation product of Fe-sulphides (mineral pyrite), which is used as lubricants in brake pads (Amato et al. 2012). Ba-sulphate of similar morphologies was found in bus PM, brake disc dust and road sediment, and thus, its origin is very likely wear of brake pads, where it is used as a filler (Grigoratos and Martini 2015).

Some phases were found only in bus PM. These phases are Ca-ferrite with minor contents of Cr, spherical Fe–Zn- and Cr–Fe-oxides, Ni-phosphide, and Sb-sulphide and metallic Sb. Ca-ferrites have been found in previous studies of snow deposits in Ljubljana, and their origin was assigned to emissions from local thermal power plants (Miler and Gosar 2009). Morphologies of spherical Fe–Zn-oxides and Cr–Fe-oxides suggest they are airborne particles that formed during melting at very high temperatures, followed by rapid cooling in the air (Piña et al. 2000). Spherical phases with similar compositions were found in snow deposits close to iron- and steel-based metallurgical industry in NNE Slovenia (Miler and Gosar 2015), but also in snow deposits from Ljubljana in the close vicinity of location 10, where possible source of spherical phases was explained by emissions from local steel casting production (Miler and Gosar 2009). Also, Teran et al. (2019) noted that in road dust in Slovenia, spherical Fe-bearing phases with Cr, Ni and Zn are more abundant in the vicinity of steel mills. Although Ni-phosphide was found only in the bus PM, its morphology and association with Cu–Zn alloy (brass) indicate that it is formed by mechanical abrasion most likely of brake pads, as brake pads can contain minor Cu–Zn alloys as reinforcing fibres (Grigoratos and Martini 2015). No reports on Ni-phosphide in PM have been found. Similarly, metallic Sb and Sb-sulphide are commonly used as a lubricant in brake pads (Amato et al. 2012; Grigoratos and Martini 2015).

Influence on human health

The main pathway for the introduction of PM into human body is inhalation. Human health can be affected by airborne PM due to both PM concentrations and physicochemical properties and pulmonary solubility of phases that the individual particles are made of.

Exposure to bus PM concentrations

Since hourly PM₁₀ and PM_{2.5} limit values are not defined, measured concentrations were compared with daily limit values, which provided only informative evaluation of measured PM concentrations. Although shorter-period measurements tend to overestimate the impact of PM concentrations with regard to daily limit values (Piringer and Schaubberger 2013; Son and Bell 2013), such approach has already been used in some studies of short-term commuter exposure to particle air pollution (e.g. Saksena et al. 2008; Kongtip et al. 2012; Keskin and Dilmac 2017). The mean PM₁₀ concentration of 82.8 µg/m³ and 81% of all measurements exceeded the daily PM₁₀ limit value of 50 µg/m³ (WHO 2006; Official Gazette RS 2011), while the mean PM_{2.5} concentration of 47.0 µg/m³ and all individual measurements exceeded the daily PM_{2.5} limit value of 25 µg/m³ (WHO 2006). The bus driver and the passengers were exposed to highest PM₁₀ and PM_{2.5} concentrations between 08:20 and 10:54 and particularly during the fifth and sixth run (between 08:48 and 10:26) (Table 2) when the mean PM₁₀ concentration was above 100 and 130 µg/m³, respectively, exceeding the daily limit value by more than 2 times. According to study of Touloumi et al. (2001), each 10 µg/m³ increment in the daily PM₁₀ concentration produces an increase in mortality of 0.62% due to short-term (daily) exposure to PM₁₀ in major European cities, including Ljubljana. This implies that the mean PM₁₀ concentration in the bus measured during the entire shift could cause between 2 and 3% increase in daily mortality risk with regard to mean ambient air PM₁₀ concentration for the studied period and mean daily ambient air PM₁₀ concentration, respectively, particularly for the bus drivers. Another study of Samet et al. (2000) showed that for each 10 µg/m³ increase in PM₁₀, there is a 2% increase in pulmonary diseases due to short-term exposure, which

again implies between 6 and 8% increase in morbidity risk for the bus drivers in our case.

Physicochemical properties and solubility of metal-bearing phases in pulmonary environment

Most of particles in bus PM are metal-bearing and 67% of them have diameters below 10 µm, and thus, it is important to study their physicochemical properties and solubility in pulmonary environment.

Theoretical solubilities of possible mineral equivalents (Fe, Ni, Cu, goethite-FeOOH, calcium ferrite-CaFe₂O₄, chromite-FeCr₂O₄, corundum-Al₂O₃, rutile-TiO₂, Sb, stibnite-Sb₂S₃ and barite-BaSO₄) of some metal-bearing phases (metallic Fe, metallic Ni, metallic Cu, Fe-oxyhydroxides, Ca-ferrites, Cr-Fe-oxides, Al-oxides, Ti-oxides, metallic Sb, Sb-sulphide and Ba-sulphate) in aqueous environment under conditions similar to those in simulated pulmonary environment (ALF) (Johnson 2003; Midander et al. 2010; Go and Jones 2016) were assessed by PHREEQC code (Parkhurst and Appelo 1999). The possible scenario was dissolution of all phases simultaneously at different Eh values. This modelling approach using PHREEQC code has already been successfully used for the assessment of solubility of metal-bearing phases in gastric environment (e.g. Miler 2017) or to demonstrate accordance of extracts obtained with simulated inhalation bioaccessibility protocols and to calculate chemical speciation and complexation in artificial lung solutions (Calas et al. 2017; Entwistle et al. 2019). It is a simplified approach as it does not consider physical properties of metal-bearing PM, organic phases and metal complexation by enzymes, which is why it could underestimate solubilities of metal-bearing phases as compared with real pulmonary environment. The simulated lung fluid ALF, used in the model, is one of the several different artificial pulmonary fluids that simulate different processes and states in different parts of lungs and are employed in most in vitro lung bioaccessibility protocols, although these protocols do not take into account effects of lipids, proteins and enzymes and are also not validated (e.g. Boisa et al. 2014; Pelfrène et al. 2017; De Miguel et al. 2019; Entwistle et al. 2019).

According to PHREEQC calculations, the most soluble phases in aqueous solution simulating pulmonary environment under both reducing (Eh = - 247 mV) and oxidising (Eh = + 247 mV) conditions

are metallic Fe, BaSO_4 and Sb_2S_3 (Fig. 8a). Metallic Fe is completely dissolved, while about 37% of BaSO_4 and 7% of Sb_2S_3 are dissolved. Al_2O_3 is also partly soluble (0.2%), while solubility of metallic Ni and TiO_2 is negligible. Other phases FeCr_2O_4 , CaFe_2O_4 , FeOOH and metallic Sb are stable and do not dissolve,

but rather precipitate from the solutions. Since Fe-oxyhydroxides (FeOOH) are a major sink for dissolved potentially toxic elements, including Cr, Zn and Cu, through co-precipitation or adsorption (Hudson-Edwards 2003; Gasparatos 2013 and references therein) and since solubility of Fe-oxyhydroxides

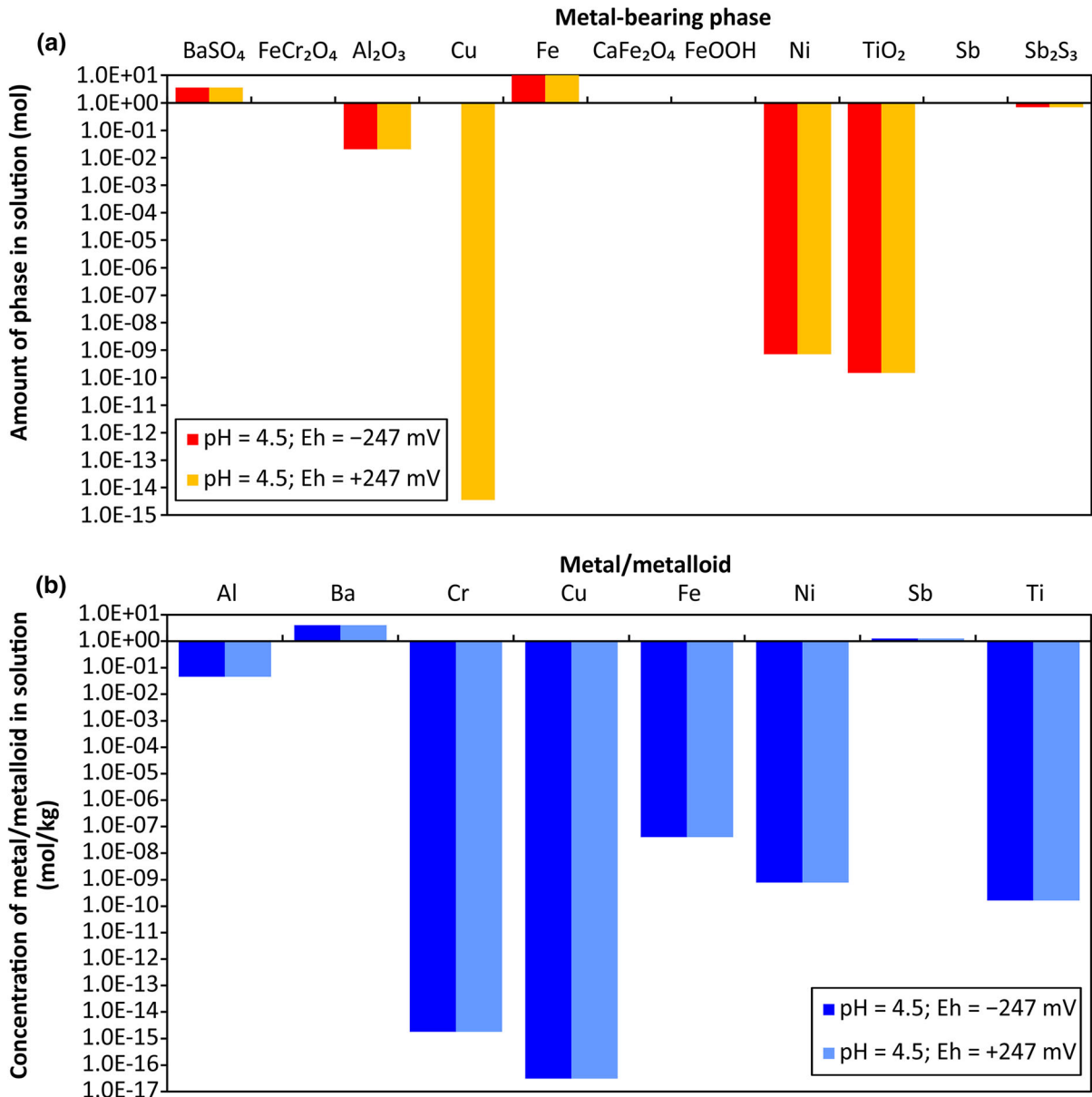


Fig. 8 Amounts of metal-bearing phases in solution (log scale) **a** and concentrations of metals and metalloids in solution **b** released from simultaneous dissolution of metal-bearing phases in aqueous solution simulating pulmonary environment (T = 37 °C; pH = 4.5; Eh = -247 and +200 mV;

$c(\text{Cl}^-) = 57.7$ mmol/l; $c(\text{Na}^+) = 209.6$ mmol/l; $c(\text{Ca}^{2+}) = 0.9$ mmol/l; $c(\text{Mg}^{2+}) = 0.5$ mmol/l; $c(\text{HPO}_4^{2-}) = 0.5$ mmol/l; $c(\text{SO}_4^{2-}) = 0.3$ mmol/l, obtained by PHREEQC calculations

generally decreases with increasing contents of impurities in these phases (Schwertmann 1991), also Fe-oxyhydroxides with minor contents of Cr, Mn, Zn, Cu and Sn can be considered stable under conditions similar to those in pulmonary environment. Metallic Cu is a specific phase, which precipitates under reducing conditions, but is slightly soluble under oxidising conditions. Stability and solubility of metal alloys could not be assessed by using PHREEQC calculations due to lack of data on these phases in PHREEQC database. According to some studies (e.g. Herting et al. 2007; Midander et al. 2010), the Cr and Ni release rates from stainless steel are generally very low in artificial lysosomal fluid (ALF), particularly from stainless steel with higher Cr and Ni content, while release of Fe is much higher. Therefore, metal alloys of Fe–Cr–Ni and Cr–Ni in our study can also be considered quite stable. The release of Cu and Ni from Ni–Cu alloys has been reported as very high in ALF (Hillwalker and Anderson 2014) and is thus considered very soluble, while the release of Cu and Zn from Cu–Zn alloy is somewhat lower (Henderson et al. 2014).

The retention time of insoluble or least soluble metal-bearing phases is thus much longer in respiratory system (e.g. Hinds 1999; Martin et al. 2014 and references therein) and could cause physical damage. However, according to their sizes, metal alloys are larger than 10 μm (Table 4) and are not considered dangerous, while Fe-oxyhydroxides, Cr–Fe-oxides, Ti-oxides and Ca-ferrites belong to PM10 fraction (Table 4) and some of them are also sharp-edged (Fe-oxyhydroxides, Ca-ferrites and Ti-oxides) and could thus act as irritants and potential carcinogens. The retention time of more soluble phases (Ba-sulphate, Al-oxide, Sb-sulphide, metallic Fe and Fe with minor contents of Cr, Ni and Cu), which are also smaller than 10 μm (Table 4), is shorter; however, released metals can pose chemical damage to human health.

The concentrations of released metals are the same both under oxidising and reducing conditions (Fig. 8b). The highest are concentrations of released Ba, Sb and also Al, while concentrations of Fe, Ni, Ti, Cr and Cu are considerably lower. Most of these released metals seem to be removed from the final solution through the in situ precipitation of secondary metal-bearing minerals and phases, which are the same under oxidising as well as reducing conditions. These secondary precipitates are represented by Al-

oxides/hydroxides, Fe-, Fe–Al-, Mg–Cr-, Ni–Fe- and Mg–Fe-spinels, Fe- and Fe–Ti-oxides, Fe-, Ni- and Cu-sulphides, and Ba-phosphate, and it can be assumed that they are stable under oxidising and reducing conditions. The newly formed secondary metal-bearing precipitates can be very small, crystal habits of some precipitates, such as Al-oxides/hydroxides and Ni-sulphides, can be unfavourable and since they are less soluble under given conditions, they can again act as irritants.

Mitigation of human exposure to PM

The study showed that buses without appropriate air intake, air conditioning or filtration systems may cause driver and passenger exposure to high concentrations of dangerous particulate matter. In order to mitigate driver and passenger exposure to PM, different measures can be undertaken. One of the more direct measures is fitting buses with improved air filtration system and changing the position of air intake, possibly to the roof of the bus. The other solution is reduction in PM emissions. This can be achieved by reducing or banning traffic in city centre that would reduce traffic congestion in city centre but would probably also cause increase in traffic levels in peripheral areas, which makes it a less effective long-term solution. A more systematic solution that would significantly reduce PM emissions and decrease human exposure in the long term and perhaps also on a more global level is enabling working from home for all employees whose jobs are suited to this mode of working. This would generally reduce the number of daily commuters that travel either by car or by other means of transportation.

Conclusions

Measurements of PM10 and PM2.5 concentrations in the bus during the entire shift (7 runs) showed that PM10 and PM2.5 concentrations were relatively low and constant with high PM2.5/PM10 ratio in the low traffic and high humidity and fog situation. In high traffic density (rush hour) with the fluid traffic flow, the PM10 and PM2.5 concentrations were much more variable and the PM2.5/PM10 ratio was much lower due to increased emissions of coarser particles caused by moving vehicles. In cases of longer traffic jams

with standing vehicles, the concentrations were lower, but the PM_{2.5}/PM₁₀ ratio was higher on the account of exhaust emissions, particularly in the strict city centre. According to obtained data, opening doors at bus stops did not affect the PM concentrations. One of the interesting observations were relatively high coarse fraction concentrations during all seven runs despite very high mean relative humidity and low mean wind speed.

The airborne particles in the bus were dominated by metal-bearing phases, represented mostly by very small-sized metal-bearing oxides/oxyhydroxides (Fe-oxyhydroxides with minor contents of Cr, Mn and Zn, Ca-ferrites with minor content of Cr, Al- and Fe–Al-oxides), relatively large metal alloys (Cu–Zn, Ni–Cu and metallic Cu with minor content of S and Ba, metallic Fe and Fe with minor contents of Cr, Ni and Cu, Fe–Cr–Ni, Cr–Ni and metallic Ni, and Ni-phosphide), and small-sized sulphides and sulphates (Sb-sulphide and Ba-sulphate). Non-metallic phases were represented by (Ca,Mg)-carbonates, Al-silicates, Na-chloride and Ca-sulphate.

The primary sources of metal-bearing oxides/oxyhydroxides were wear of brake discs, brake pads and tyres (Fe-oxyhydroxides with minor contents of Cr, Mn, Zn, Cu and Sn), but also wear of engine and catalytic converters (Al- and Fe–Al-oxides), emissions from local thermal power plants (Ca-ferrites), and abrasion of road marking paint (Ti-oxides). Metal alloys originated from wear of brake discs and brake pads and also exhaust emissions (wear of engine components and catalytic converters). The main source of sulphides and sulphates was wear of brake pads. Non-metallic phases originated mostly from resuspension of road sediment, which contained road sanding materials, but also from vehicle emissions of burned fuel and lubricating oil (Ca-sulphate).

The study of exposure to PM concentrations showed that the mean PM₁₀ and PM_{2.5} concentrations exceeded daily limit values and that they could cause 2–3% increase in daily mortality risk and 6–8% increase in morbidity risk for the bus drivers with regard to mean ambient air PM₁₀ concentration for the studied period and mean daily ambient air PM₁₀ concentration. Simplified PHREEQC calculations of solubility of airborne metal-bearing phases in aqueous environment simulating pulmonary environment showed that metallic Fe, Ba-sulphate (BaSO₄), Sb-sulphide (Sb₂S₃) and partly Al-oxide (Al₂O₃) were the

most soluble phases under reducing and oxidising conditions resulting in release of Ba, Sb and also Al. However, most of released metals were removed from the solution through re-precipitation of stable secondary metal-bearing phases. Cu-bearing metal alloys were also considered soluble, while other phases were stable. Since this is a modelling approach that does not take into account effects of all factors, it could underestimate solubilities of metal-bearing phases as compared with real pulmonary environment.

Acknowledgements The author acknowledges financial support from the state budget by the Slovenian Research Agency obtained through the research projects “Source identification of solid pollutants in the environment on the basis of mineralogical, morphological and geochemical properties of particles” (No. Z1-7187) and “Dynamics and matter flow of potentially toxic elements (PTEs) in urban environment” (No. J1-1713), and programme “Mineral resources” (No. P1-0025). The author is also thankful to Ljubljana public transport (LPP d.o.o.) for enabling measurements and sampling, and to the editor and two anonymous reviewers for the thorough revision of the manuscript and their constructive comments that helped improve the paper.

References

- Adams, H. S., Nieuwenhuijsen, M. J., & Colvile, R. N. (2001). Determinants of fine particle (PM_{2.5}) personal exposure levels in transport microenvironments, London UK. *Atmospheric Environment*, *35*, 4557–4566.
- Adams, H. S., Nieuwenhuijsen, M. J., Colvile, R. N., Older, M. J., & Kendall, M. (2002). Assessment of road users’ elemental carbon personal exposure levels, London, UK. *Atmospheric Environment*, *36*, 5335–5342.
- Alm, S., Jantunen, M. J., & Vartiainen, M. (1999). Urban commuter exposure to particle matter and carbon monoxide inside and automobile. *Journal of Exposure Analysis and Environmental Epidemiology*, *9*, 237–244.
- Amato, F., Font, O., Moreno, N., Alastuey, A., & Querol, X. (2012). Mineralogy and elemental composition of brake pads of common use in Spain. *Macla*, *16*, 154–156.
- Anderson, J. O., Thundiyil, J. G., & Stolbach, A. (2012). Clearing the air: A review of the effects of particulate matter air pollution on human health. *Journal of Medical Toxicology*, *8*, 166–175.
- Anthony, J. W., Bideaux, R. A., Bladh, K. W., & Nichols, M. C. (2009). The Handbook of Mineralogy. Mineralogical Society of America. <https://www.handbookofmineralogy.org/>. Accessed 28 October 2019.
- Barthelmy, D. (2010). The Mineralogy Database. <https://webmineral.com/>. Accessed 28 October 2019.
- Bell, M. L., & Holloway, T. (2007). Global impacts of particulate matter air pollution. *Environmental Research Letters*, *2*(4), 045026.

- Bernstein, L. S., Lang, R. J., Lunt, R. S., Musser, G. S., & Fedor, R. J. (1973). Nickel-copper alloy No_x reduction catalysts for dual catalyst systems. *SAE Transactions*, 82, 1930–1942.
- Boisa, N., Elom, N., Dean, J. R., Deary, M. E., Bird, G., & Entwistle, J. A. (2014). Development and application of an inhalation bioaccessibility method (IBM) for lead in the PM_{10} size fraction of soil. *Environment International*, 70, 132–142.
- Boogaard, H., Borgman, F., Kamminga, J., & Hoek, G. (2009). Exposure to ultrafine and fine particles and noise during cycling and driving in 11 Dutch cities. *Atmospheric Environment*, 43, 4234–4242.
- Breed, C. A., Arocena, J. M., & Sutherland, D. (2002). Possible sources of PM_{10} in Prince George (Canada) as revealed by morphology and in situ chemical composition of particulate. *Atmospheric Environment*, 36, 1721–1731.
- Calas, A., Uzu, G., Martins, J. M. F., Voisin, D., Spadini, L., Lacroix, T., et al. (2017). The importance of simulated lung fluid (SLF) extractions for a more relevant evaluation of the oxidative potential of particulate matter. *Scientific Reports*, 7, 11617. <https://doi.org/10.1038/s41598-017-11979-3>
- Cepeda, M., Schoufour, J., Freak-Poli, R., Koolhaas, C. M., Dhana, K., Bramer, W. M., et al. (2017). Levels of ambient air pollution according to mode of transport: A systematic review. *The Lancet Public Health*, 2(1), e23–e34.
- Chan, L. Y., Lau, W. L., Lee, S. C., & Chan, C. Y. (2002). Commuter exposure to particulate matter in public transportation modes in Hong Kong. *Atmospheric Environment*, 36, 3363–3373.
- Chen, Y., Shah, N., Huggins, F. E., & Huffman, G. P. (2006). Microanalysis of ambient particles from Lexington, KY, by electron microscopy. *Atmospheric Environment*, 40, 651–663.
- Correia, C., Martins, V., Cunha-Lopes, I., Faria, T., Diapouli, E., Eleftheriadis, K., et al. (2020). Particle exposure and inhaled dose while commuting in Lisbon. *Environmental Pollution*, 257, 113547. <https://doi.org/10.1016/j.envpol.2019.113547>
- Dallmann, T. R., Onasch, T. B., Kirchstetter, T. W., Worton, D. R., Fortner, E. C., Herndon, S. C., et al. (2014). Characterization of particulate matter emissions from on-road gasoline and diesel vehicles using a soot particle aerosol mass spectrometer. *Atmospheric Chemistry and Physics*, 14, 7585–7599.
- Davis, H. T., Aelion, C. M., McDermott, S., & Lawson, A. B. (2009). Identifying natural and anthropogenic sources of metals in urban and rural soils using GIS-based data, PCA, and spatial interpolation. *Environmental Pollution*, 157, 2378–2385.
- De Miguel, E., Ordóñez, A., Barrio-Parra, F., Izquierdo-Díaz, M., Álvarez, R., Mingot, J., et al. (2019). Bioaccessibility of trace elements in urban environments. In S. M. Charlesworth & C. A. Booth (Eds.), *Urban pollution: Science and management* (1st ed., pp. 107–118). Hoboken: Wiley.
- Deng, Q., Deng, L., Miao, Y., Guo, X., & Li, Y. (2019). Particle deposition in the human lung: Health implications of particulate matter from different sources. *Environmental Research*, 169, 237–245.
- Entwistle, J. A., Hursthouse, A. S., Marinho Reis, P. A., & Stewart, A. G. (2019). Metalliferous mine dust: Human health impacts and the potential determinants of disease in mining communities. *Current Pollution Reports*, 5, 67–83.
- Evans, A., & Evans, R. (2006). *The Composition of a tyre: Typical components*. Banbury: The Waste and Resources Action Programme.
- Gasparatos, D. (2013). Sequestration of heavy metals from soil with Fe–Mn concretions and nodules. *Environmental Chemistry Letters*, 11, 1–9.
- Gehrig, R., & Buchmann, B. (2003). Characterising seasonal variations and spatial distribution of ambient PM_{10} and $\text{PM}_{2.5}$ concentrations based on long-term Swiss monitoring data. *Atmospheric Environment*, 37, 2571–2580.
- Gieré, R., & Querol, X. (2010). Solid particulate matter in the atmosphere. *Elements*, 6(4), 215–222.
- Gilmour, P. S., Brown, D. M., Lindsay, T. G., Beswick, P. H., MacNee, W., & Donaldson, K. (1996). Adverse health effects of PM_{10} particles: involvement of iron in generation of hydroxyl radical. *Occupational and Environmental Medicine*, 53, 817–822.
- Girard, J. E. (2010). *Principles of environmental chemistry* (2nd ed.). Sudbury: Jones and Bartlett Publishers.
- Go, Y. M., & Jones, D. P. (2016). Exposure memory and lung regeneration. *American Thoracic Society*, 13(Suppl. 2), S452–S461.
- Gokul Raj, M., & Karthikeyan, S. (2020). Effect of modes of transportation on commuters' exposure to fine particulate matter ($\text{PM}_{2.5}$) and nitrogen dioxide (NO_2) in Chennai, India. *Environmental Engineering Research*, 25(6), 898–907.
- Goldstein, J., Newbury, D., Joy, D., Lyman, C., Echlin, P., Lifshin, E., et al. (2003). *Scanning electron microscopy and x-ray microanalysis* (3rd ed.). New York: Kluwer Academic/Plenum Publishers.
- Gottesfeld, P. (2015). Time to ban lead in industrial paints and coatings. *Frontiers in Public Health*, 3, 144. <https://doi.org/10.3389/fpubh.2015.00144>.
- Grigoratos, T., & Martini, G. (2015). Brake wear particle emissions: A review. *Environmental Science and Pollution Research*, 22, 2491–2504.
- Grobéty, B., Gieré, R., Dietze, V., & Stille, P. (2010). Airborne particles in the urban environment. *Elements*, 6(4), 229–234.
- Hamanaka, R. B., & Mutlu, G. M. (2018). Particulate matter air pollution: Effects on the cardiovascular system. *Frontiers in Endocrinology*, 9, 680. <https://doi.org/10.3389/fendo.2018.00680>.
- Henderson, R. G., Verougstraete, V., Anderson, K., Arbildua, J. J., Brock, T. O., Brouwers, T., et al. (2014). Inter-laboratory validation of bioaccessibility testing for metals. *Regulatory Toxicology and Pharmacology*, 70, 170–181.
- Herting, G., Odnevall Wallinder, I., & Leygraf, C. (2007). Metal release from various grades of stainless steel exposed to synthetic body fluids. *Corrosion Science*, 49, 103–111.
- Hillwalker, W. E., & Anderson, K. A. (2014). Bioaccessibility of metals in alloys: Evaluation of three surrogate biofluids. *Environmental Pollution*, 185, 52–58.
- Hinds, W. C. (1999). *Aerosol technology: Properties, behavior, and measurement of airborne particles* (2nd ed.). New York: Wiley.

- Hodzic, A., Madronich, S., Bohn, B., Massie, S., Menut, L., & Wiedinmyer, C. (2007). Wildfire particulate matter in Europe during summer 2003: meso-scale modeling of smoke emissions, transport and radiative effects. *Atmospheric Chemistry and Physics*, 7, 4043–4064.
- Hudson-Edwards, K. A. (2003). Sources, mineralogy, chemistry and fate of heavy metal-bearing particles in mining-affected river systems. *Mineralogical Magazine*, 67, 205–217.
- JEOL. (2007). *JSM-6490LV scanning electron microscope, instruction manual*. Tokyo: JEOL Ltd.
- Johnson, L. R. (2003). *Essential medical physiology* (3rd ed.). San Diego: Academic Press.
- Kaiser, M. S., & Dutta, S. (2014). Wear behavior of commercial aluminium engine block and piston under dry sliding condition. *International Journal of Chemical, Molecular, Nuclear, Materials and Metallurgical Engineering*, 8(8), 860–865.
- Karanasiou, A., Viana, M., Querol, X., Moreno, T., & de Leeuw, F. (2014). Assessment of personal exposure to particulate air pollution during commuting in European cities—recommendations and policy implications. *Science of the Total Environment*, 490, 785–797.
- Kaur, S., Nieuwenhuijsen, M. J., & Colville, R. N. (2007). Fine particulate matter and carbon monoxide exposure concentrations in urban street transport microenvironments. *Atmospheric Environment*, 41, 4781–4810.
- Keskin, S. S., & Dilmac, E. (2017). Indoor air particulate matter exposure of commuter bus passengers in Istanbul Turkey. *Indoor and Built Environment*, 26(3), 337–346.
- Khan, I., Saeed, K., & Khan, I. (2019). Nanoparticles: Properties, applications and toxicities. *Arabian Journal of Chemistry*, 12(7), 908–931.
- Kim, K.-H., Kabir, E., & Kabir, S. (2015). A review on the human health impact of airborne particulate matter. *Environment International*, 74, 136–143.
- Kongtip, P., Anthayanon, T., Yoosook, W., & Onchoi, C. (2012). Exposure to particulate matter, CO₂, CO, VOCs among bus drivers in Bangkok. *Journal of the Medical Association of Thailand*, 95(Suppl. 6), S169–S178.
- Krsmanović, R. (2003). Characterization and analysis of heavy metal particles in fly ashes from oil-fired power stations by scanning electron microscopy. *Microscopia Elettronica*, 24(1), 94–105.
- Kukutschová, J., Moravec, P., Tomášek, V., Matějka, V., Smolík, J., Schwarz, J., et al. (2011). On airborne nano/micro-sized wear particles released from low-metallic automotive brakes. *Environmental Pollution*, 159(4), 998–1006.
- Kumar, P., Rivas, I., Singh, A. P., Ganesh, V. J., Ananya, M., & Frey, H. C. (2018). Dynamics of coarse and fine particle exposure in transport microenvironments. *npj Climate and Atmospheric Science*, 1, 11. <https://doi.org/10.1038/s41612-018-0023-y>.
- Kupiaainen, K., Ritola, R., Stojiljkovic, A., Pirjola, L., Malinen, A., & Niemi, J. (2016). Contribution of mineral dust sources to street side ambient and suspension PM₁₀ samples. *Atmospheric Environment*, 147, 178–189.
- Lin, H., Ratnapradipa, K., Wang, X., Zhang, Y., Xu, Y., Yao, Z., et al. (2017). Hourly peak concentration measuring the PM_{2.5}-mortality association: Results from six cities in the Pearl River delta study. *Atmospheric Environment*, 161, 27–33.
- Makino, H. (2018). Safety of nanoparticles. In M. Naito, T. Yokoyama, K. Hosokawa, & K. Nogi (Eds.), *Nanoparticle technology handbook* (3rd ed., pp. 379–388). Amsterdam: Elsevier.
- Martin, R., Dowling, K., Pearce, D., Sillitoe, J., & Florentine, S. (2014). Health effects associated with inhalation of airborne arsenic arising from mining operations. *Geosciences*, 4, 128–175.
- McNabola, A., Broderick, B. M., & Gill, L. W. (2008). Relative exposure to fine particulate matter and VOCs between transport microenvironments in Dublin: Personal exposure and uptake. *Atmospheric Environment*, 42, 6496–6512.
- Midander, K., de Frutos, A., Hedberg, Y., Darrie, G., & Odnevall Wallinder, I. (2010). Bioaccessibility studies of ferrochromium alloy particles for a simulated inhalation scenario. A comparative study with the pure metals and stainless steel. *Integrated Environmental Assessment and Management*, 6(3), 441–455.
- Miler, M. (2014). SEM/EDS characterisation of dusty deposits in precipitation and assessment of their origin. *Geologija*, 57(1), 5–14.
- Miler, M. (2017). Characterisation of secondary metal-bearing phases in used dental amalgam and assessment of gastric solubility. *Environmental Geochemistry and Health*, 39, 1607–1619.
- Miler, M., & Gosar, M. (2009). Characterisation of solid airborne particles in urban snow deposits from Ljubljana by means of SEM/EDS. *RMZ – Materials and Geoenvironment*, 56(3), 266–282.
- Miler, M., & Gosar, M. (2013). Assessment of metal pollution sources by SEM/EDS analysis of solid particles in snow: A case study of Žerjav, Slovenia. *Microscopy and Microanalysis*, 19, 1606–1619.
- Miler, M., & Gosar, M. (2015). Chemical and morphological characteristics of solid metal-bearing phases deposited in snow and stream sediment as indicators of their origin. *Environmental Science and Pollution Research*, 22, 1906–1918.
- Mills-Knapp, S., Traore, K., Ericson, B., Keith, J., Hanrahan, D., & Caravanos, J. (2012). *The world's worst pollution problems: Assessing health risks at hazardous waste sites*. New York: Blacksmith Institute.
- Miri, M., Ebrahimi Aval, H., Ehrampoush, M. H., Mohammadi, A., Toolabi, A., Nikonahad, A., et al. (2017). Human health impact assessment of exposure to particulate matter: An AirQ software modeling. *Environmental Science and Pollution Research*, 24, 16513–16519.
- Moreno, T., Reche, C., Rivas, I., Cruz Mingüillón, M., Martins, V., Vargas, C., et al. (2015). Urban air quality comparison for bus, tram, subway and pedestrian commutes in Barcelona. *Environmental Research*, 142, 495–510.
- Mudge, S. M. (2008). Environmental forensics and the importance of source identification. In R. E. Hester & R. M. Harrison (Eds.), *Environmental forensics* (pp. 1–16). Cambridge: Royal Society of Chemistry.
- Naidoo, S., & Steyn, W. J. vdM. (2018). Performance of thermoplastic road-marking material. *Journal of the South African Institution of Civil Engineering*, 60(2), 9–22.

- Ny, M. T., & Lee, B. K. (2011). Size distribution of airborne particulate matter and associated metallic elements in an urban area of an industrial city in Korea. *Aerosol and Air Quality Research*, *11*, 643–653.
- Odekanle, E. L., Fakinle, B. S., Akeredolu, F. A., Sonibare, J. A., & Adesanmi, A. J. (2016). Personal exposures to particulate matter in various modes of transport in Lagos city Nigeria. *Cogent Environmental Science*, *2*(1), 1260857. <https://doi.org/10.1080/23311843.2016.1260857>
- Official Gazette, R. S. (2011). Decree on ambient air quality (in Slovene). *Official Gazette of the Republic of Slovenia*, *911*, 964–983.
- Okuda, T., Katsuno, M., Naoi, D., Nakao, S., Tanaka, S., He, K., et al. (2008). Trends in hazardous trace metal concentrations in aerosols collected in Beijing, China from 2001 to 2006. *Chemosphere*, *72*, 917–924.
- Onat, B., & Stakeeva, B. (2013). Personal exposure of commuters in public transport to PM_{2.5} and fine particle counts. *Atmospheric Pollution Research*, *4*, 329–335.
- Oxford Instruments. (2006). *INCA energy operator manual*. High Wycombe: Oxford Instruments Analytical Ltd.
- Parkhurst, D. L., & Appelo, C. A. J. (1999). *Users' guide to PHREEQC (Version 2)—a computer program for speciation, batch-reaction, one-dimensional transport, and inverse geochemical calculations*. Denver: U.S. Geological Survey.
- Pelfrène, A., Cave, M. R., Wragg, J., & Douay, F. (2017). In vitro investigations of human bioaccessibility from reference materials using simulated lung fluids. *International Journal of Environmental Research and Public Health*, *14*(2), 112. <https://doi.org/10.3390/ijerph14020112>
- Piña, A. A., Torres, G. V., Monroy, M. F., Luszczewski, A. K., & Leyva, R. R. (2000). Scanning electron microscope and statistical analysis of suspended heavy metal particles in San Luis Potosi, Mexico. *Atmospheric Environment*, *34*, 4103–4112.
- Piringer, M., & Schaubberger, G. (2013). Dispersion modelling for odour exposure assessment. In V. Belgiorno, V. Nadeo, & T. Zarra (Eds.), *Odour impact assessment handbook* (pp. 125–174). Chichester: Wiley.
- Ravindra, K., Bencs, L., & Van Grieken, R. (2004). Platinum group elements in the environment and their health risk. *Science of the Total Environment*, *318*, 1–43.
- Rist, S., & Hartmann, N. B. (2017). Aquatic ecotoxicity of microplastics and nanoplastics: Lessons learned from engineered nanomaterials. In M. Wagner & S. Lambert (Eds.), *Freshwater microplastics: Emerging environmental contaminants?* (pp. 25–49). Cham: Springer Nature.
- Rodríguez, S., Alastuey, A., Alonso-Pérez, S., Querol, X., Cuevas, E., Abreu-Afonso, J., et al. (2011). Transport of desert dust mixed with North African industrial pollutants in the subtropical Saharan air layer. *Atmospheric Chemistry and Physics*, *11*, 6663–6685.
- Saha Podder, A., & Bhanja, A. (2013). Applications of stainless steel in automobile industry. *Advanced Materials Research*, *794*, 731–740.
- Saksena, S., Quang, T. N., Nguyen, T., Dang, P. N., & Flachsbar, P. (2008). Commuters' exposure to particulate matter and carbon monoxide in Hanoi Vietnam. *Transportation Research Part D*, *13*, 206–211.
- Samet, J. M., Zeger, S. L., Dominici, F., Curriero, F., Coursac, I., Dockery, D. W., et al. (2000). The national morbidity, mortality, and air pollution study. Part II: Morbidity and mortality from air pollution in the United States. *Research Reports of the Health Effects Institute*, *94*, 5–70.
- Schöner, W., Staudinger, M., Winiwarter, W., & Pichlmayer, F. (1993). Dating of snow samples from snow pits at sonnblück austrian alps as a tool for interpretation of chemical analysis. In P. M. Borell, P. Borell, T. Cvtas, & W. Seiler (Eds.), *The Proceedings of EUROTRAC Symposium '92* (pp. 753–756). The Hague: SPB Academic Publishing.
- Schwertmann, U. (1991). Solubility and dissolution of iron oxides. *Plant and Soil*, *130*(1–2), 1–25.
- Setti, L., Passarini, F., De Gennaro, G., Barbieri, P., Pallavicini, A., Ruscio, M., et al. (2020). Searching for SARS-COV-2 on particulate matter: A possible early indicator of COVID-19 epidemic recurrence. *International Journal of Environmental Research and Public Health*, *17*(9), E2986. <https://doi.org/10.3390/ijerph17092986>
- Slanina, S. (2006). Impact of local air pollution. In J. Cutler (Ed.), *Encyclopedia of Earth*. Washington, D.C.: Environmental Information Coalition, National Council for Science and the Environment. https://www.eoearth.org/article/Impact_of_local_air_pollution. Accessed 6 March 2011.
- Slovenian Environment Agency. (2015). Air quality from automatic monitoring stations. https://www.arso.gov.si/zrak/kakovost%20zraka/podatki/amp/e00_t_30.html. Accessed 9 April 2015.
- Slovenian Environment Agency. (2019). Archive of meteorological data. <https://meteo.arso.gov.si/met/si/app/webmet/#webmet==8Sdwx2bhR2cv0WZ0V2bvEGcw9ydIJWblR3LwVnaz9SYtVmYh9icIFGbt9SaulGdugXbsx3cs9mdl5WahxXYyNGapZXZ8tHZv1WYp5mOnMHbvZXZulWYnwCchJXYtVGdlJnOn0UQQdSf>. Accessed 1 December 2019.
- Son, J. Y., & Bell, M. L. (2013). The relationships between short-term exposure to particulate matter and mortality in Korea: Impact of particulate matter exposure metrics for sub-daily exposures. *Environmental Research Letters*, *8*(1), 014015.
- Sun, Y., Hub, X., Wu, W., Lian, H., & Chen, Y. (2014). Fractionation and health risks of atmospheric particle-bound as and heavy metals in summer and winter. *Science of the Total Environment*, *493*, 487–494.
- Šeme Lesjak, Š. (2014). *Winter maintenance of state roads* (in Slovene). Ljubljana, Slovenia: B&B higher vocational college. https://www.bb.si/doc/diplome/Seme_Lesjak_Spela.pdf
- Teran, K., Žibret, G., & Fanetti, M. (2019). Impact of urbanization and steel mill emissions on elemental composition of street dust and corresponding particle characterization. *Journal of Hazardous Materials*, *384*, 120963. <https://doi.org/10.1016/j.jhazmat.2019.120963>
- Thompson, J. E. (2018). Airborne particulate matter: Human exposure and health effects. *Journal of Occupational and Environmental Medicine*, *60*(5), 392–423.
- Touloumi, G., Samoli, E., Gryparis, A., Le Tertre, A., Monopoli, Y., et al. (2001). Confounding and effect modification in the short-term effects of ambient particles on total

- mortality: Results from 29 European cities within the APHEA2 project. *Epidemiology*, *12*, 521–531.
- Tsai, D. H., Wu, Y. H., & Chan, C. C. (2008). Comparisons of commuter's exposure to particulate matters while using different transportation modes. *Science of the Total Environment*, *405*, 71–77.
- van Setten, B. A. A. L., Makkee, M., & Moulijn, J. A. (2001). Science and technology of catalytic diesel particulate filters. *Catalysis Reviews*, *43*(4), 489–564.
- von Glasow, R., Bobrowski, N., & Kern, C. (2009). The effects of volcanic eruptions on atmospheric chemistry. *Chemical Geology*, *263*, 131–142.
- Wang, L., Stanič, S., Bergant, K., Eichinger, W., Močnik, G., & Drinovec, L. (2019). Retrieval of vertical mass concentration distributions—Vipava valley case study. *Remote Sensing*, *11*(2), 106. <https://doi.org/10.3390/rs11020106>
- WHO (2006). Air quality guidelines for particulate matter, ozone, nitrogen dioxide and sulfur dioxide. Global update 2005. Summary of risk assessment. https://apps.who.int/iris/bitstream/10665/69477/1/WHO_SDE_PHE_OEH_06_02_eng.pdf. Accessed 1 December 2019.
- Wikipedia contributors. (2018). City bus service no. 6 (Ljubljana). Wikipedia, The Free Encyclopedia. [https://en.wikipedia.org/w/index.php?title=City_bus_service_no._6_\(Ljubljana\)&oldid=874013961](https://en.wikipedia.org/w/index.php?title=City_bus_service_no._6_(Ljubljana)&oldid=874013961). Accessed 23 September 2019.
- Wu, W., Jin, Y., & Carlsten, C. (2018). Inflammatory health effects of indoor and outdoor particulate matter. *Journal of Allergy and Clinical Immunology*, *141*(3), 833–844.
- Xie, R. K., Seip, H. M., Liu, L., & Zhang, D. S. (2009). Characterization of individual airborne particles in Taiyuan city, China. *Air Quality, Atmosphere and Health*, *2*, 123–131.
- Yu, X., O'Connell, M., Hu, J., Tanrikulu, S., Soon, S.-T., Tran, C., et al. (2019). Regional sources of airborne ultrafine particle number and mass concentrations in California. *Atmospheric Chemistry and Physics*, *19*, 14677–14702.
- Zurbier, M., Hoek, G., Oldenwening, M., Lenters, V., Meliefste, K., van den Hazel, P., et al. (2010). Commuters' exposure to particulate matter air pollution is affected by mode of transport, fuel type, and route. *Environmental Health Perspectives*, *118*(6), 783–789.

Publisher's Note Springer Nature remains neutral with regard to jurisdictional claims in published maps and institutional affiliations.